THE JOURNAL OF BIOLOGICAL CHEMISTRY VOL. 291, NO. 23, pp. 12208–12222, June 3, 2016


# Caveolin-1 Regulates the $P2Y_2$ Receptor Signaling in Human 1321N1 Astrocytoma Cells*

Received for publication, March 31, 2016, and in revised form, April 15, 2016 Published, JBC Papers in Press, April 18, 2016, DOI 10.1074/jbc.M116.730226

**Namyr A. Martinez[‡1], Alondra M. Ayala[§], Magdiel Martinez[‡], Freddyson J. Martinez-Rivera[¶], Jorge D. Miranda[‡], and Walter I. Silva[‡2]**

*From the Departments of [‡]Physiology and Biophysics, [§]Psychiatry, and [¶]Anatomy and Neurobiology, School of Medicine, University of Puerto Rico, Medical Sciences Campus, San Juan, Puerto Rico 00936*

**Damage to the CNS can cause a differential spatio-temporal release of multiple factors, such as nucleotides, ATP and UTP. The latter interact with neuronal and glial nucleotide receptors. The $P2Y_2$ nucleotide receptor ($P2Y_2R$) has gained prominence as a modulator of gliotic responses after CNS injury. Still, the molecular mechanisms underlying these responses in glia are not fully understood. Membrane-raft microdomains, such as caveolae, and their constituent caveolins, modulate receptor signaling in astrocytes; yet, their role in $P2Y_2R$ signaling has not been adequately explored. Hence, this study evaluated the role of caveolin-1 (Cav-1) in modulating $P2Y_2R$ subcellular distribution and signaling in human 1321N1 astrocytoma cells. Recombinant $hP2Y_2R$ expressed in 1321N1 cells and Cav-1 were found to co-fractionate in light-density membrane-raft fractions, co-localize via confocal microscopy, and co-immunoprecipitate. Raft localization was dependent on ATP stimulation and Cav-1 expression. This $hP2Y_2R$/Cav-1 distribution and interaction was confirmed with various cell model systems differing in the expression of both $P2Y_2R$ and Cav-1, and shRNA knockdown of Cav-1 expression. Furthermore, shRNA knockdown of Cav-1 expression decreased nucleotide-induced increases in the intracellular $Ca^{2+}$ concentration in 1321N1 and C6 glioma cells without altering TRAP-6 and carbachol $Ca^{2+}$ responses. In addition, Cav-1 shRNA knockdown also decreased AKT phosphorylation and altered the kinetics of ERK1/2 activation in 1321N1 cells. Our findings strongly suggest that $P2Y_2R$ interaction with Cav-1 in membrane-raft caveolae of 1321N1 cells modulates receptor coupling to its downstream signaling machinery. Thus, $P2Y_2R$/Cav-1 interactions represent a novel target for controlling $P2Y_2R$ function after CNS injury.**

Neurodegenerative conditions are among the leading causes of death and disability in the United States and have dramatically increased in incidence during the last decade (1, 2). The P2 receptors for extracellular nucleotides have emerged as key modulators of the pathophysiology of neurodegeneration (3–6). G protein-coupled $P2Y_2$ nucleotide receptors ($P2Y_2Rs$)[3] have been identified in both neurons and glia as mediators of pro-inflammatory responses, neurotransmission, apoptosis, proliferation, and cell migration (3–5, 7, 8). In addition, the $P2Y_2Rs$ have also gained prominence, due to their association with some types of neoplasms, spinal cord injury, and the enhancement of neuronal differentiation (7, 9–15). Further insight into the spatio-temporal organization of the $P2Y_2R$ and its signaling cascades in astrocytic cells is required to expand our knowledge of their role in neurodegenerative diseases. In this context, evidence suggests that receptors and associated signaling molecules are not randomly distributed in plasma membranes but are localized in specialized membrane microdomains, namely membrane rafts (MRs), such as caveolae (Cav) (16–20). MRs are specialized membrane domains enriched in cholesterol and glycosphingolipids (21), which are known to localize signaling molecules, including several types of receptors (*e.g.* receptor protein kinases and heptahelical receptors), G protein subunits, and an array of signaling molecules (22–25). These scaffolds serve to facilitate protein-protein interactions among signaling molecules, thereby integrating complex signaling pathways.

Recently, we have reviewed and established the importance of glial caveolins and the caveolar MR compartment in neurodegenerative conditions, such as Alzheimer disease, aging, among others (26, 27). Caveolin-1 (Cav-1), one of the main raft scaffolding proteins (26, 28–31), has been shown to modulate multiple cellular responses by coupling membrane receptors to downstream signaling molecules (28–32). Because $P2Y_2R$ expression in 1321N1 astrocytoma cells has been shown to exert glio-protective and neurotrophic actions (33–35), analysis of the subcellular and molecular mechanisms involved in its actions deserve special attention. Although the precise endocytic mechanism of the $P2Y_2R$ has been partially characterized (36–39), the functional significance of $P2Y_2R$ trafficking in MRs is only beginning to be recognized (36, 40, 41). Therefore, this study was undertaken to assess the potential role of Cav-1 in modulating $P2Y_2R$ subcellular distribution and signaling in 1321N1 astrocytoma cells. Results obtained indicate that $P2Y_2R$ resides in Cav-1 raft microdomains and their interaction

* This work was supported, in part, by Centers of Biomedical Research Excellence COBRE Grant P20-GM103642 at the University of Puerto Rico-Medical Sciences Campus (UPR-MSC). The content is solely the responsibility of the authors and does not necessarily represent the official views of the National Institutes of Health. The authors declare that they have no conflicts of interest with the contents of this article.

[1] Supported by the National Institutes of Health, NIGMS MBRS-RISE Program Grant R25GM061838 at the UPR-MSC and also the Associate Deanship of Biomedical Sciences of the UPR-MSC.

[2] To whom correspondence should be addressed: P. O. Box 365067, San Juan, Puerto Rico 00936-5067. Tel.: 787-751-2042; Fax: 787-767-3139; E-mail: walter.silva@upr.edu.

[3] The abbreviations used are: $P2Y_2R$, $P2Y_2$ nucleotide receptor; MRs, membrane rafts; Cav-1, caveolin-1; SCRAM, scrambled; KD, knockdown; PCRA, primary cultures of rat astrocytes; IP, immunoprecipitation; ANOVA, analysis of variance.

regulates P2Y$_2$R signal transduction by extracellular ATP, including intracellular calcium mobilization and Akt and ERK1/2 activities. Together, our results suggest that the interaction between P2Y$_2$R and Cav-1 in raft microdomains is a key factor mediating nucleotide signaling in astrocytic cells regulating their protective, trophic, and degenerative functions in the CNS.

## Experimental Procedures

*Antibodies and Reagents*—The following antibodies and reagents were used in this study: anti-phospho-Akt (Ser$^{473}$) (D9E) (1:2000), anti-Akt (pan) (C67E7) (1:1000), anti-phospho-p44/42 MAPK (ERK1/2) (Thr$^{202}$/Tyr$^{204}$, D13.14.4E) (1:2000), and anti-total p44/42 MAPK (ERK1/2) (1:1000) antibodies from Cell Signaling Technology (Boston, MA); anti-hemagglutinin (HA) (3F10 and 12CA5) (1:500) antibodies from Roche Applied Science (Indianapolis, IN); anti-P2Y2 receptor antibody (1:400) from Alomone Labs (Jerusalem, Israel); mouse monoclonal anti-flotillin-2 (1:500) and mouse monoclonal anti-caveolin-1 (1:1000) from BD Biosciences (San Jose, CA); rabbit polyclonal anti-caveolin-1 (1:7500), anti-flotillin-2 (1:500), anti-GAPDH (1:10000), mouse monoclonal anti-FLAG M2-HRP (1:1000), mouse IgG-agarose beads, Protein A-HRP, anti-FLAG M2 Magnetic Beads, and anti-$\alpha$-tubulin clone B-5-1-2 (1:5000) from Sigma; horseradish peroxidase-conjugated goat anti-mouse IgG, goat anti-rabbit IgG, rabbit anti-mouse IgG1, and rabbit anti-mouse IgG2a secondary antibodies were obtained from NeuroMab (UC Davis/NIH NeuroMab Facility); and Alexa Fluor-488 goat anti-mouse IgG and Alexa Fluor-633 goat anti-mouse IgG secondary antibodies from Molecular Probes (Eugene, OR). ATP, TRAP-6, and carbamylcholine were obtained from Tocris Bioscience (Ellisville, MO). Fetal bovine serum, fura-2-acetoxymethyl ester (fura-2AM), Pluronic F-127, Probenecid (water soluble), and ProLong Gold Antifade Reagent were purchased from Life Technologies. Control (SC108080), human caveolin-1 (SC29241), and rat caveolin-1 (SC106996) shRNA Lentiviral Particles, anti-c-Myc (9E10) agarose affinity gel, c-Myc antibody (9E10) HRP (1:1000), normal rabbit IgG agarose affinity gel, normal mouse IgG agarose affinity gel, normal rabbit IgG, and normal mouse IgG were purchased from Santa Cruz Biotechnology (Santa Cruz, CA). All other reagents, unless mentioned, were obtained from Sigma.

*Cell Culture*—Wild type (WT) human 1321N1 astrocytoma cells devoid of functional P2 receptors, pLXSN 1321N1 astrocytoma cells, and human N-terminal HA-tagged P2Y$_2$R expressing 1321N1 astrocytoma cells were a kind gift from Dr. Gary A. Weisman, University of Missouri (33, 42–44). WT human 1321N1 astrocytoma cells were grown at 37 °C in a humidified 5% $CO_2$ atmosphere in Dulbecco's modified Eagle's medium (DMEM) supplemented with 5% (v/v) FBS (Life Technologies Corp.), 100 units/ml of penicillin, and 100 mg/ml of streptomycin. To express human HA-tagged P2Y$_2$R (hHAP2Y$_2$R) in this cell line, the retroviral vector pLXSN was used, as previously described (42, 43). Human 1321N1 cells expressing hHAP2Y$_2$R (hHAP2Y$_2$R 1321N1) or the empty vector pLXSN (pLXSN 1321N1) were grown as above, but in the presence of 500 $\mu$g/ml of G418, and cells were infected with Cav-1 or scrambled shRNA-containing lentiviral particles in the presence of 5 $\mu$g/ml of puromycin dihydrochloride. C6 rat glioma and HEK-293 cells (CCL-107 and CRL-1573, American Type Culture Collection, Manassas, VA) were grown in Ham's F-12K or DMEM containing 10% (v/v) FBS (Life Technologies Corp.), 100 units/ml of penicillin, and 100 mg/ml of streptomycin, respectively (45). Cells infected with either Cav-1 or scrambled shRNA-containing lentiviral particles were supplemented with 5 $\mu$g/ml of puromycin dihydrochloride. The immortalized mouse microglial cells (BV-2) were originally obtained from Dr. R. Donato (University of Perugia, Italy) and cultured in DMEM containing 10% (v/v) FBS (Life Technologies Corp.), 100 units/ml of penicillin, and 100 mg/ml of streptomycin (46). Primary cultures of rat astrocytes (PCRA) (obtained from the NIH-NCRR-RCMI supported Neuronal Glia Culture Facility of Universidad Central del Caribe School of Medicine, Bayamón, PR) were grown in DMEM containing 10% FBS, 100 units/ml of penicillin, and 100 mg/ml of streptomycin (27).

*Treatments*—When indicated, cells were incubated in serum-free medium for 16–24 h prior to treatments. For time course experiments, cells were treated with 100 $\mu$M ATP or 100 $\mu$M UTP in serum-free medium for 5, 10, 15, 30, or 60 min. Serum-free medium-treated cells served as controls (vehicle or untreated).

*shRNA Lentiviral Infection*—Cells were infected with either control shRNA lentiviral particles (scrambled or non-targeted shRNA) or caveolin-1 shRNA-containing lentiviral particles obtained from Santa Cruz Biotechnology, following the manufacturer's recommendations. After infection, stable cell clones expressing the shRNA constructs were isolated by selection with 5 $\mu$g/ml of puromycin dihydrochloride.

*Measurement of the Intracellular Calcium Concentration, $[Ca^{2+}]_i$*—Changes in $[Ca^{2+}]_i$ were measured using the $Ca^{2+}$-sensitive fluorescent ratiometric dye fura-2. Cells were seeded 16–24 h before experiments in clear flat-bottom black 96-well culture trays (Corning Life Sciences, Corning, NY) at a density of $3.0 \times 10^4$ cells/well. The medium was removed and replaced with HEPES-buffered saline (HBS; 5 mM KCl, 145 mM NaCl, 10 mM D-glucose, 1 mM $MgCl_2$, 1 mM $CaCl_2$, 10 mM HEPES, and 0.1% (w/v) bovine serum albumin (BSA), pH 7.4) containing 5 $\mu$M fura-2AM and 0.05% (w/v) Pluronic F-127, and cells were incubated for 1 h at room temperature in the dark. The loaded cells were washed twice with HBS and covered with 200 $\mu$l of HBS supplemented with 2.5 mM probenecid for at least 20 min at room temperature to allow for fura-2AM de-esterification. Fluorescence emission intensity at 510 nm was determined in individual wells using a plate reader equipped with an automated injection system (Infinite M200 Pro, Tecan, Männedorf, Switzerland) at alternating excitation wavelengths of 340 and 380 nm every 3 s for 60 acquisition cycles (cycle, 3 s; exposure, 25 flashes; gain, 120) in response to agonists added with the automated injector. $[Ca^{2+}]_i$ in cells was expressed as the average emission at 510 nm in individual wells in response to excitation at 340/380 nm normalized to initial fluorescence emission obtained during the first 10–20 cycles. Analysis of the resulting phramacodynamic parameters from the nucleotide-mediated dose-response curves is described under "Statistical Analysis."

*Detergent-free Purification of Caveolin-rich Membrane Fractions*—Discontinuous sucrose density gradients were prepared as previously described (27, 45, 47) with minor modifications. In brief, cells were grown to 70–80% confluence in two 150-mm dishes, serum-starved for 16–24 h, treated with DMEM or Ham's F-12K (basal/vehicle) or with DMEM or Ham's F-12K supplemented with 100 $\mu$M ATP or UTP for 30 min and then washed with ice-cold MES-buffered saline (25 mM MES, 150 mM NaCl, pH 6.0). Cells were then scraped from dishes and homogenized in 2.0 ml of 500 mM sodium carbonate, pH 11, supplemented with 1% (v/v) protease inhibitor mixture (Sigma) and 1% (v/v) phosphatase inhibitor mixture 3 (Sigma). Homogenization was carried out sequentially at 4 °C using a loose fitting Dounce homogenizer (15 strokes), then a sonicator (Sonic Dismembrator System, Model 120; Fisher Scientific, Cayey, PR) at mid power (three 20-s bursts interposed by 60 s of rest). Homogenates were then adjusted for equal protein loading and discontinuous sucrose density gradients were prepared. Samples were centrifuged at 100,000 × *g* for 22 h in a SW 40Ti rotor (Beckman Coulter, Fullerton, CA). Twelve gradient fractions were collected (1 ml/each), washed with MBS, and centrifuged in an 80Ti rotor (Beckman Coulter) at 100,000 × *g* for 30 min. The resulting pellets were resuspended in urea sample buffer (USB) (62 mM Tris-HCl, pH 6.8, 4% (w/v) SDS, 8 M urea, 20 mM EDTA, 5% (v/v) mercaptoethanol, and 0.015% (w/v) bromphenol blue), boiled, and equal sample volumes were resolved on 10–12% SDS-PAGE gels.

*Protein Extraction*—Cells were washed with ice-cold PBS, and lysed with CelLytic M Mammalian Cell Lysis/Extraction Reagent, supplemented with 1% protease mixture with phosphatase inhibitor, as above. Extracts were maintained with constant agitation for 30 min at 4 °C and then centrifuged for 20 min at 17,000 × *g*. Supernatants were collected and used to determine total protein concentration using the Bradford Quick-Start Protein Assay (Bio-Rad).

*Expression Constructs and DNA Transfections*—N-terminal FLAG-tagged human P2Y$_2$R expression vector was constructed using recombinant cDNA synthesized by IDT (Integrated DNA Technologies, Inc., IA) and cloned into pcDNA3.1 mammalian expression vector (Invitrogen) by the standard PCR extension overlap technique (48). Construct identity was confirmed by sequencing, and functionality was tested in 1321N1 cells. The C-terminal Myc-tagged human caveolin-1 pcDNA3.1 expression vector was kindly provided by Dr. Jeffrey E. Pessin, Stony Brook University, New York, NY (49). HEK-293 cells were seeded in 10-cm plates (3.0 × 10$^6$ cells/plate) overnight in DMEM, 10% FBS, and 1% antibiotic/antimycotic (Sigma) at 37 °C. For the transient expression of the different constructs, cells were transfected with 6 $\mu$g of empty pcDNA3.1, pcDNA3.1/Myc-caveolin-1, pcDNA3.1/FLAG-P2Y$_2$R, or cotransfected with 3 $\mu$g of pcDNA3.1/Myc-caveolin-1 and 3 $\mu$g of pcDNA3.1/FLAG-P2Y$_2$R using X-tremeGENE HP DNA transfection reagent (Roche Molecular Biochemicals) according to the manufacturer's instructions. After 36 h, cells were washed with PBS and changed to essentially serum-free DMEM (0.5% FBS) and incubated for another 16 h at 37 °C for further experiments.

*Immunoprecipitation Assays*—Serum-starved (16–24 h) confluent cultures of hHAP2Y$_2$R 1321N1 and pLXSN 1321N1 astrocytoma cells were washed twice with ice-cold PBS and lysed for 45 min at 4 °C in IP lysis buffer A (50 mM Tris, pH 8.0, 150 mM NaCl, 5 mM EDTA, 1% Triton X-100, 60 mM octyl glucoside, and complete protease and phosphatase inhibitors). Subsequently, lysates were centrifuged at 13,000 × *g* for 12 min at 4 °C. In other assays, serum-starved (16–24 h) confluent cultures of hHAP2Y$_2$R 1321N1 were DMEM (vehicle) or DMEM with 100 $\mu$M ATP treated and prepared as above. To immunoprecipitate the hHAP2Y$_2$R, the Pierce HA Tag IP/Co-IP kit was used as directed by the manufacturer (Thermo Scientific, Rockford, IL). Briefly, 600 $\mu$g of cell lysates were mixed with 20 $\mu$l of anti-HA-agarose beads and added to spin columns. Samples were incubated overnight at 4 °C with end-over-end mixing, and then the immunocomplexes were washed three times with lysis buffer A and twice with lysis buffer B (50 mM Tris, pH 8.0, 150 mM NaCl, 5 mM EDTA). C6 rat glioma cells, primary cultures of rat astrocytes, and transiently transfected HEK-293 cells expressing pcDNA3.1, pcDNA3.1/Myc-caveolin-1, pcDNA3.1/FLAG-P2Y$_2$R, pcDNA3.1/Myc-caveolin-1, and pcDNA3.1/FLAG-P2Y$_2$R were washed twice each with cold PBS and lysed for 45 min at 4 °C in IP lysis buffer A. Lysates were then centrifuged and supernatants were pre-cleared with mouse IgG-agarose beads (Sigma) for 1 h at 4 °C. After centrifugation, supernatants were collected and protein concentration was determined using the BCA protein assay kit (Thermo Fisher Scientific Inc.). Equal amounts of total proteins ~500 $\mu$g were incubated with either 1 $\mu$g of mouse monoclonal anti-cav-1 antibody (BD Biosciences, San Jose, CA) and 30 $\mu$l of Protein A/G Magnetic Beads (Thermo Scientific, Rockford, IL), with anti-FLAG M2 Magnetic Beads (Sigma) or with Anti-c-Myc (9E10) Agarose Affinity Gel (Santa Cruz Biotechnology) for 4 h at 4 °C with end-over-end rotation. All samples were resuspended in Laemmli buffer (0.2 M Tris-HCl, pH 6.8, 2% SDS, 10% glycerol, 0.01% bromphenol blue, 20 mM DTT) with subsequent mixing and incubation at 65 °C for 15 min. Samples were then separated on 10–12% SDS-PAGE, transferred to nitrocellulose membranes, and immunoblotted with the appropriate antibodies.

*SDS-PAGE and Immunoblot Analysis*—Both were performed as previously described (47) with modifications. Equal amounts of whole cell protein extracts were suspended in 6× Laemmli sample buffer (0.375 M Tris, pH 6.8, 12% (w/v) SDS, 60% (v/v) glycerol, 0.6 M DTT, 0.06% (w/v) bromphenol blue, and 8 M urea), then heated and electrophoresed on Pre-Cast TGX-SDS gels (Bio-Rad). Proteins in the gel were transferred to nitrocellulose membranes using the Bio-Rad Turbo Trans-Blot apparatus at preprogrammed recommended settings. Membranes were blocked with 5% (w/v) nonfat milk in TBST (25 mM Tris-HCl, pH 7.4, 150 mM NaCl, and 0.1% (v/v) Tween 20) for 1 h at 22 °C and the appropriate primary antibodies were added overnight at 4 °C. Membranes were then washed with TBST and probed with the corresponding horseradish peroxidase-conjugated IgG secondary antibody (1:15,000) at 22 °C for 1 h. Membranes were washed several times with TBST and blots were developed using an ECL kit (SuperSignal Femto, Pierce). All images were obtained using a Bio-Rad VersaDoc 4000 Sys-

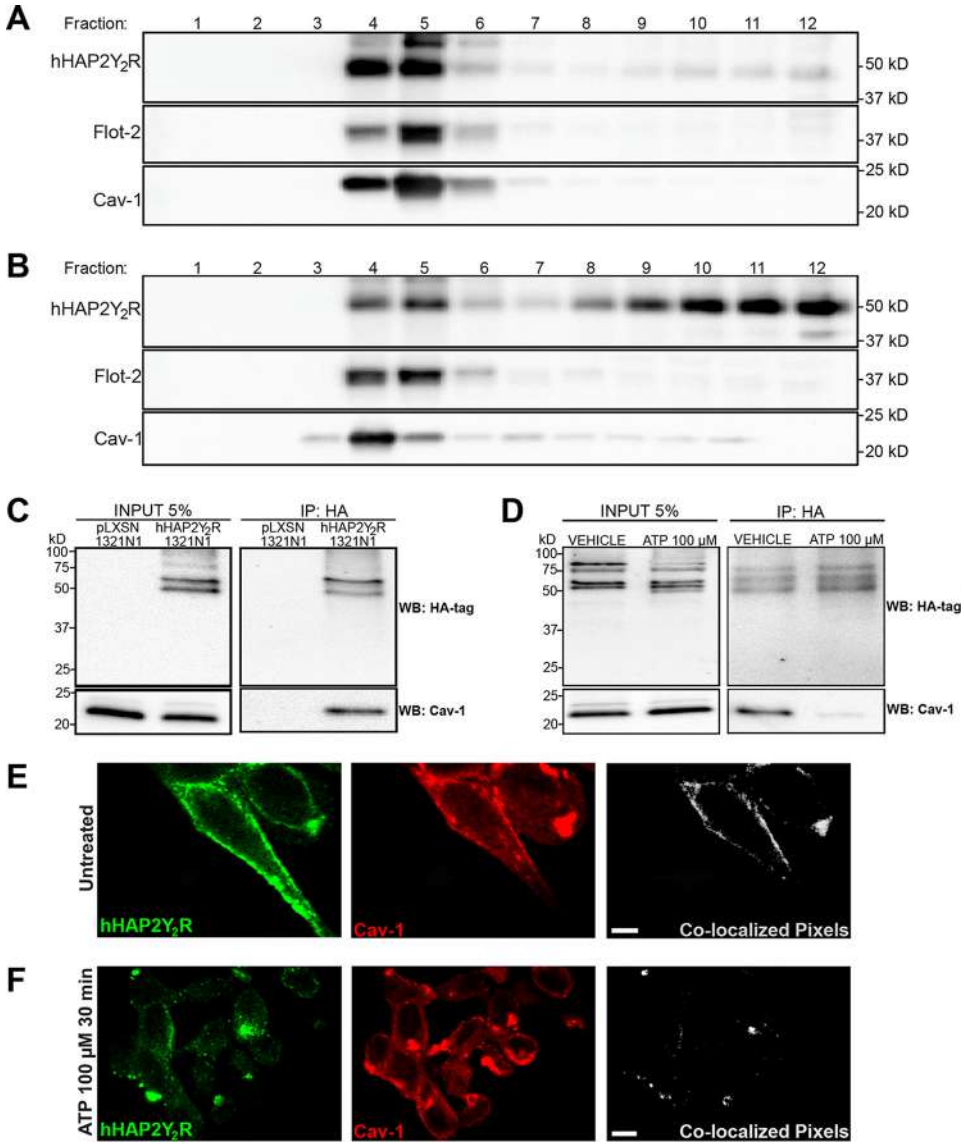


FIGURE 1. **Activation of the P2Y$_2$ receptor changes its subcellular distribution and decreases interactions with caveolin-1 in 1321N1 astrocytoma cells.** *A* and *B*, detergent-free sucrose density gradient fractionation of homogenates from serum-starved hHAP2Y$_2$ 1321N1 cells (*A*) untreated or (*B*) treated with 100 $\mu$M ATP for 30 min analyzed by immunoblotting using primary anti-HA (*hHAP2Y$_2$R*), anti-flotillin-2 (*Flot-2*), or anti-caveolin-1 (*Cav-1*) antibodies. *C* and *D*, hHAP2Y$_2$R was immunoprecipitated using homogenates from serum-starved hHAP2Y$_2$R 1321N1 cells untreated (*C*) or treated (*D*) with 100 $\mu$M ATP for 30 min with anti-HA-conjugated agarose beads. IP of lysates from pLXSN 1321N1 cells was performed as a control. Western blot (*WB*) analysis using anti-Cav-1 and anti-HA antibodies indicates co-IP of the hHAP2Y$_2$R and Cav-1, and that this interaction is agonist dependent. *E* and *F*, laser scanning confocal microscopy of serum-starved hHAP2Y$_2$R 1321N1 cells untreated (*E*) or treated (*F*) with 100 $\mu$M ATP for 30 min. Secondary antibodies detected the hHAP2Y$_2$R are shown in *green* (Alex Fluor 488 dye) and caveolin-1 shown in *red* (Alexa Fluor 633 dye) and co-localization between the two dyes is shown in *gray*. Representative images from over 20 cells were examined for each condition are shown. *Scale bar* indicates 20 $\mu$m. All results shown are representative of 3–4 independent experiments.

tem, as previously described (27) and densitometric analysis was done using NIH ImageJ software. To reprobe with different antibodies, the membranes were first stripped using Restore PLUS Western blot Stripping Buffer (Thermo Scientific) at 22 °C for 30 min, washed extensively, reblocked with 5% (w/v) nonfat milk in TBST and then incubated with the appropriate antibodies.

*Immunofluorescent Staining*—$1 \times 10^4$ cells/well were seeded and grown on 4-well laboratory Tek chamber slides II (Thermo Scientific) for 3 days, and equilibrated in serum-free DMEM for at least 16 h at 37 °C. Cells were washed with cold HBS and nonspecific protein sites were blocked with a mixture of 0.1% (w/v) BSA and 1% (v/v) normal goat serum in HBS for 15 min at 4 °C (blocking buffer), followed by an incubation with 10 $\mu$g/ml of anti-HA 12CA5 mouse monoclonal antibody in blocking buffer for 1 h at 4 °C to form receptor-antibody complexes (44, 50). Cells were washed with ice-cold HBS and incubated with or without 100 $\mu$M ATP in HBS at 37 °C for 30 min. Cells were then washed with ice-cold HBS and fixed with 1% (v/v) formaldehyde (Electron Microscopy Sciences, Hatfield, PA), in 0.1 M phosphate-buffered saline for 10 min at room temperature, followed by permeabilization with 0.1% (w/v) saponin, 1% (w/v) BSA, 1% (v/v) normal goat serum in PBS. The HA-tagged receptors were detected by incubation with Alexa Fluor 488-conjugated goat anti-mouse IgG antibody. Cav-1 was detected using a polyclonal rabbit primary antibody

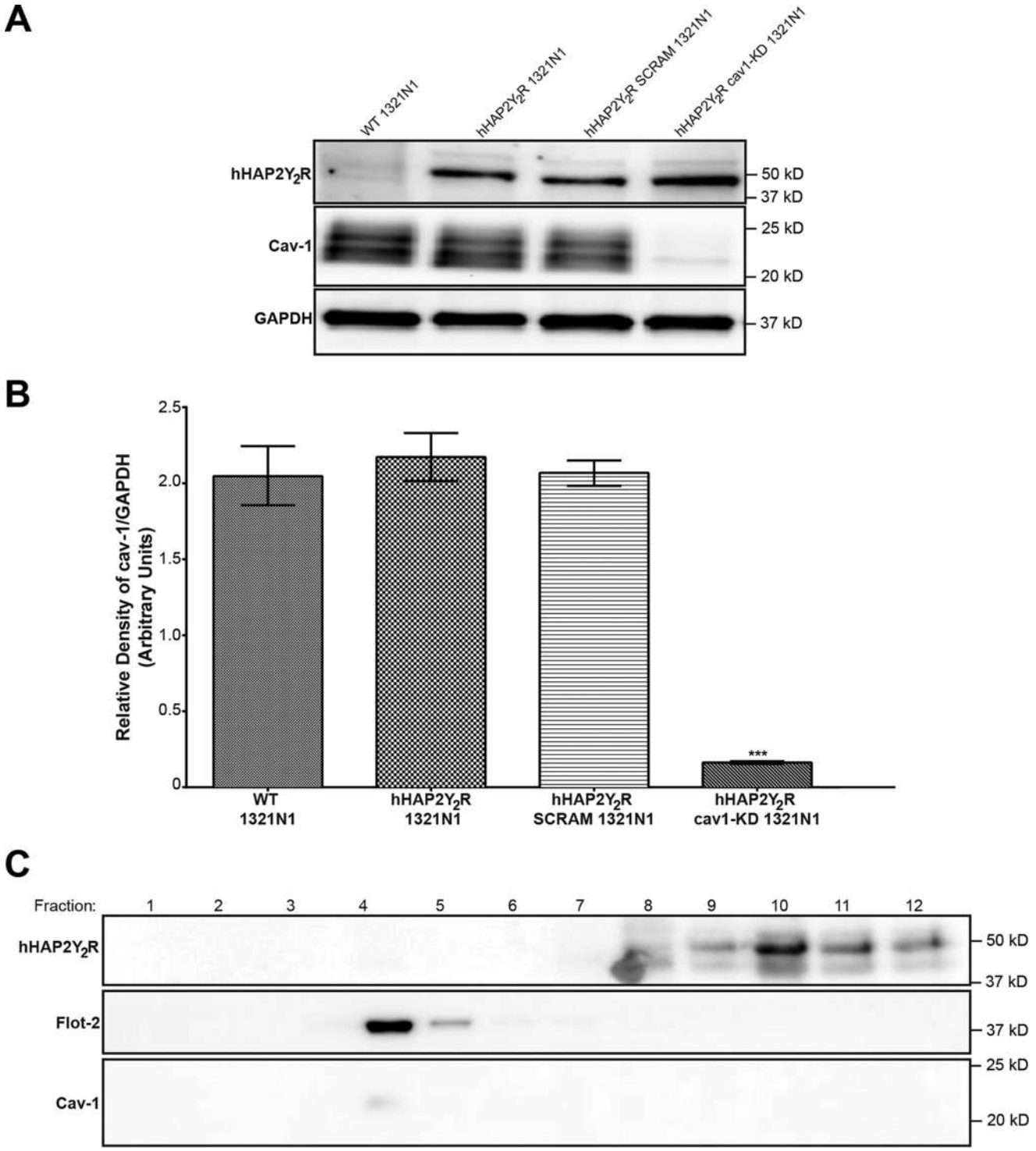


FIGURE 2. **shRNA-mediated knockdown of caveolin-1 expression causes redistribution of the P2Y$_2$R from membrane rafts.** *A,* immunoblot analysis of hHAP2Y$_2$R, Cav-1, and GAPDH (control) expression in serum-starved WT 1321N1 cells (*lane 1*) or hHAP2Y$_2$R 1321N1 cells (*lanes 2–4*) before (*lane 2*) or after infection with scrambled (SCRAM) shRNA (*lane 3*) or Cav-1 shRNA (*lane 4*; Cav-1 KD) lentiviral particles. *B*, densitometric analysis of immunoblots indicates the level of Cav-1 normalized to GAPDH expression. Results are presented as the mean ± S.E. ($n = 3$; ***, $p < 0.001$ as determined by one-way ANOVA). *C,* Cav-1 KD was performed in hHAP2Y$_2$R 1321N1 cells and homogenates subjected to detergent-free sucrose density gradient fractionation. All fractions were immunoblotted and analyzed, as described in the legend to Fig. 1. hHAP2Y$_2$R dissociates from the raft or buoyant fraction in the absence of Cav-1. The data shown are representative of 3–4 independent experiments.

(1:150) and Alexa Fluor 633-conjugated goat anti-rabbit IgG antibody. Slides were washed and mounted using the Prolong Gold Antifade Kit (Molecular Probes) according to the manufacturer's protocol. Laser scanning confocal microscopy was performed as described in Ref. 27. Briefly, a Zeiss LSM510 Confocal Microscope equipped with a ×63 oil-immersion objective, a 488 nm argon/2 laser, a 633 He/Ne laser, and a BP 500–550 or LP 650 filter was used for image acqui-

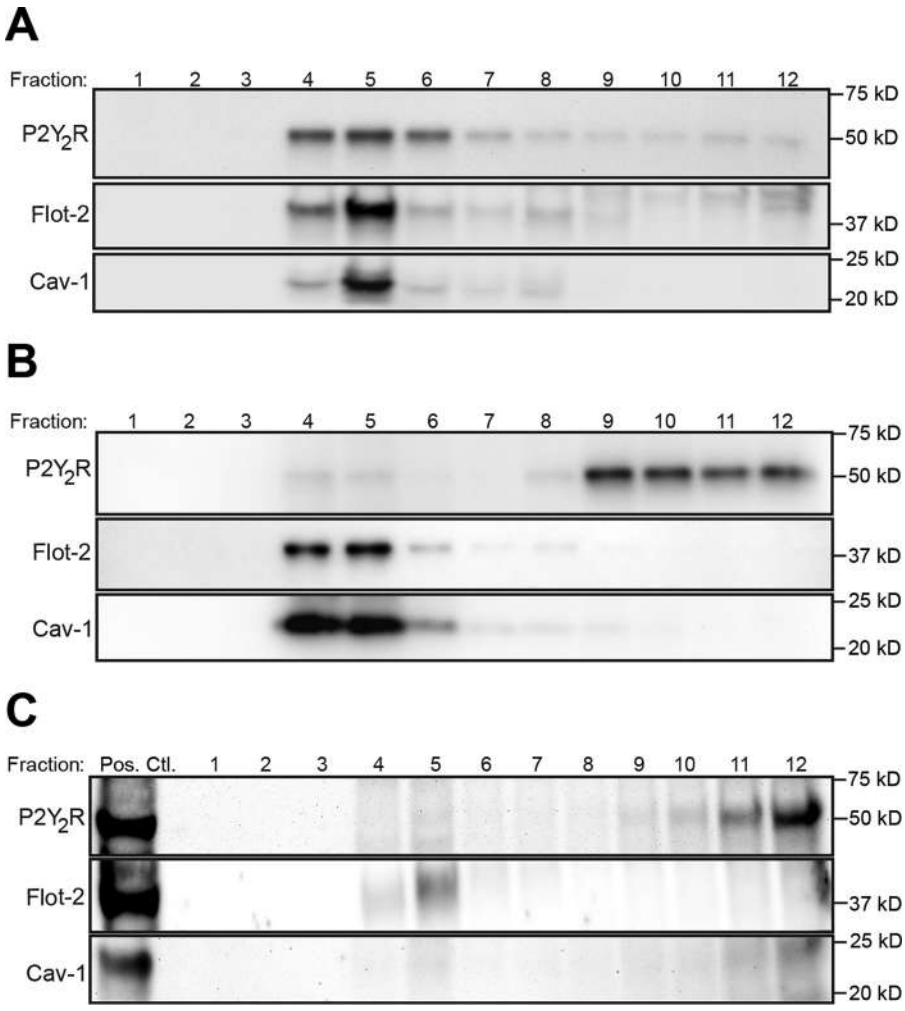


FIGURE 3. **The P2Y$_2$R subcellular distribution is also dependent on agonist activation in C6 rat glioma and absence of caveolin-1 in BV-2 microglial cells.** These experiments were done on C6 glioma cells, which endogenously express P2Y$_2$R and Cav-1, and BV-2, which are Cav-1 devoid. *A* and *B*, detergent-free sucrose density gradient fractionation of homogenates from serum-starved C6 rat glioma cells untreated (*A*) or treated (*B*) with 100 $\mu$M UTP for 30 min and analyzed by immunoblotting using primary anti-P2Y$_2$R, anti-flotillin-2 (*Flot-2*), or anti-caveolin-1 (*Cav-1*) antibodies. *C*, sucrose density gradient fractionation of BV-2 cells. BV-2 cell homogenates were subjected to detergent-free sucrose density gradient fractionation, and all fractions plus a Cav-1 positive control were immunoblotted and analyzed. The distribution of the P2Y$_2$R across the BV-2 fractions was similar to that of the Cav-1 KD hHAP2Y$_2$R 1321N1, being present mostly in the non-raft or heavy fractions. Results shown are representative of 3–4 independent experiments.

sition and images were analyzed with CoLocalizer Pro software version 2.7.1 (51, 52).

*Statistical Analysis*—Mean values of treatment data from at least four independent experiments were calculated and expressed as a percentage of mean values from untreated controls (which were set to 100%). One-way ANOVA followed by multiple Tukey comparison post-test or unpaired Student's *t* test was used for comparison of multiple groups or two groups, respectively. A *p* value less than 0.05 between control and experimental groups was considered to be statistically significant. All analyses were performed using GraphPad Prism, version 6.0e for Mac OS X (GraphPad Software Inc., San Diego, CA). Pharmacodynamic parameters ($E_{max}$ and $EC_{50}$) for nucleotide-mediated dose-response curves for calcium flux in 1321N1 and C6 cells were calculated using the Michaelis-Menten equation in GraphPad Prism. Maximal responses were normalized for each cell line assigning the maximal calcium responses for hHAP2Y$_2$R 1321N1 and wild type C6 controls an intrinsic activity value of 1.0, respectively. Parameter data were expressed as mean ± S.E. of at least 3 independent experiments and were subjected to unpaired Student's *t* test. Differences between mean values were considered significant when $p < 0.05$.

## Results

*The hHAP2Y$_2$R Localization in Cav-1 Membrane Raft Microdomains Is Modulated by ATP in Human 1321N1 Astrocytoma Cells*—Demonstration of membrane raft residence demands the use of a series of complementary experimental approaches; particularly, subcellular co-fractionation, confocal imaging co-localization, and co-immunoprecipitation. As a first approach, sucrose density gradient centrifugation under detergent-free conditions was performed to explore the possibility of co-fractionation of the hHAP2Y$_2$R with the MR protein Cav-1 in 1321N1 cells (Fig. 1). Under basal conditions, hHAP2Y$_2$R co-fractionates with Cav-1, as determined by immunoblot analysis of light density MR fractions 4–6 that express raft marker proteins Cav-1 and flotillin-2 (Flot-2) (Fig.

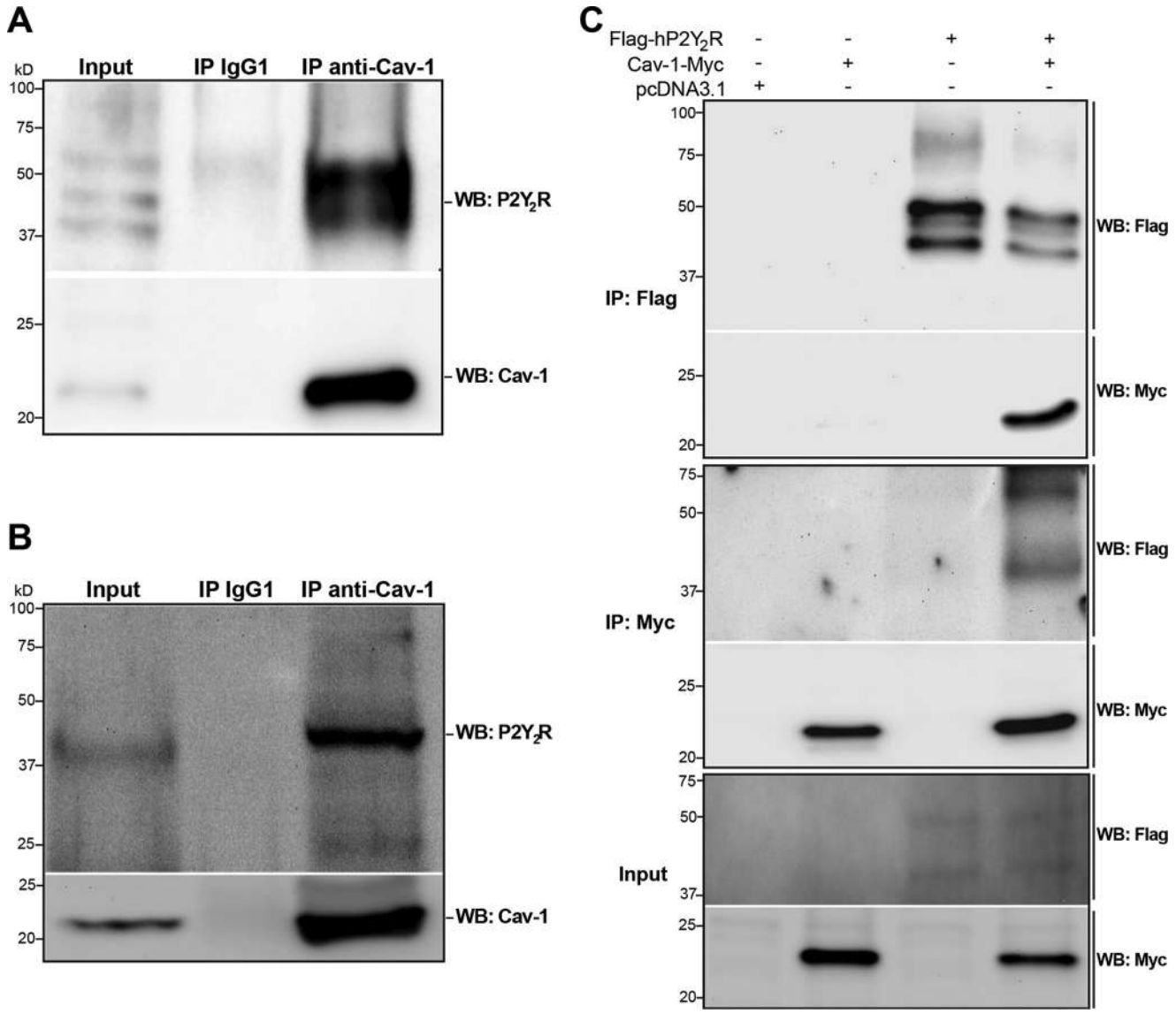


FIGURE 4. **Cav-1 interacts with P2Y$_2$ receptors in C6 glioma cells, primary cultures of rat astrocytes and HEK-293 cells.** Western blot (*WB*) analysis of C6 glioma cells (*A*) and PCRA (*B*) lysates show that endogenously expressed P2Y$_2$ receptors were IP by mouse monoclonal Cav-1 antibody and protein A/G-magnetic beads (*3rd lane*) but not with non-immune control mouse IgG1 antibody and protein A/G-magnetic beads (*2nd lane*). The *first lane* shows detection of Cav-1 and P2Y$_2$R from total C6 and PCRA cell lysates used (~20 $\mu$g). Polyclonal rabbit anti-Cav-1 and anti-P2Y$_2$R antibodies were used for Western blot detection. *C,* Western blot from HEK-293 cells transiently transfected with empty pcDNA3.1, pcDNA3.1 Myc-caveolin-1, pcDNA3.1 Flag-P2Y$_2$R or cotransfected with pcDNA3.1 Myc-caveolin-1 and pcDNA3.1 Flag-P2Y$_2$R. Cells were incubated for at least 16 h with essentially serum-free DMEM (1% FBS). Lysates were prepared and subjected to immunoprecipitation using either anti-FLAG M2 Magnetic Beads (*IP: Flag*) or anti-c-Myc (9E10) Agarose Affinity Gel (*IP: Myc*) ("Experimental Procedures"). The *3rd panel from the top (Input*) shows Western blot detection of Myc-Cav-1 and FLAG-P2Y$_2$ receptors from total lysates used (~20 $\mu$g). Monoclonal HRP-conjugated anti-FLAG and anti-Myc antibodies were used for Western blot detection. Representative Western blot from a single experiment that has been replicated three times with equivalent results are shown.

1*A*). Activation of the hHAP2Y$_2$R with 100 $\mu$M ATP for 30 min induced a significant increase in the distribution of the P2Y$_2$R to the high density, non-buoyant fractions 8–12 that were devoid of Cav-1 and Flot-2 (Fig. 1*B*). hHAP2Y$_2$R interactions with Cav-1 under basal conditions were definitively demonstrated by co-immunoprecipitation of hHAP2Y$_2$R and Cav-1 (Fig. 1*C*). This interaction was also found to be agonist sensitive, as addition of ATP (100 $\mu$M) for 30 min reduced the co-immunoprecipitation of the hHAP2Y$_2$R with Cav-1 (Fig. 1*D*). Immunofluorescence microscopy showed that Cav-1 co-localizes with the hHAP2Y$_2$R under basal conditions (Fig. 1*E*) and addition of 100 $\mu$M ATP also decreases hHAP2Y$_2$R/Cav-1 co-localization (Fig. 1*F*). These findings strongly suggest that hHAP2Y$_2$R interacts directly with Cav-1 under basal conditions and that activation of hHAP2Y$_2$R causes its dissociation from Cav-1 and plasma MR in 1321N1 astrocytoma cells.

*Knockdown (KD) of Cav-1 Expression Causes Redistribution of the P2Y$_2$R from Membrane Rafts*—To validate the role of Cav-1 in hHAP2Y$_2$R distribution to low density buoyant plasma MRs, we decreased Cav-1 expression in hHAP2Y$_2$ 1321N1 cells using Cav-1 shRNA-containing lentiviral particles. Western blot analysis indicated that Cav-1 expression was decreased by Cav-1 shRNA, but not scrambled (SCRAM) shRNA, in hHAP2Y$_2$ 1321N1 cells (Fig. 2*A*). When normalized to GAPDH, Cav-1 KD in hHAP2Y$_2$ 1321N1 cells decreased Cav-1 expression by ~80–85%, as compared with untreated

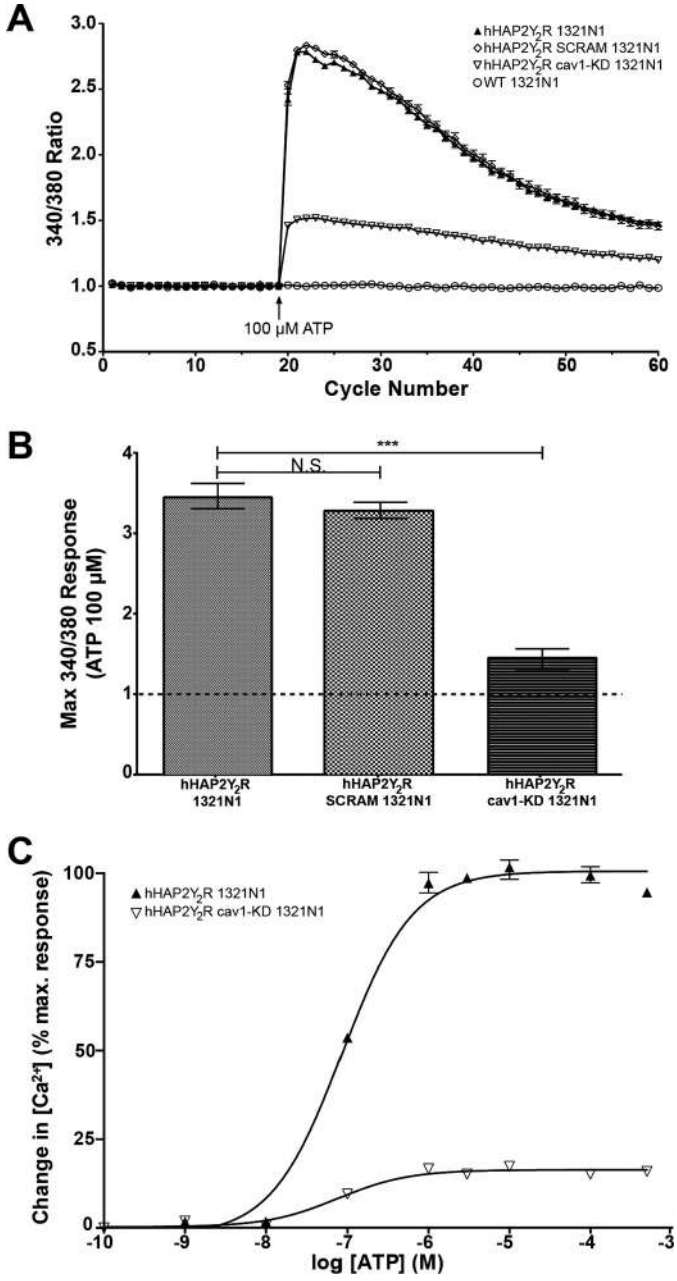


FIGURE 5. **Knockdown of caveolin-1 by shRNA inhibits P2Y$_2$R-mediated intracellular $Ca^{2+}$ $[Ca^{2+}]_i$ signaling in 1321N1 cells.** *A,* representative traces of intracellular calcium responses to 100 $\mu$M ATP in serum-starved WT 1321N1 cells, hHAP2Y$_2$R 1321N1 cells, hHAP2Y$_2$R cav1-KD 1321N1 cells, and hHAP2Y$_2$R 1321N1 cells infected with scrambled shRNA ($n = 5$). *B,* maximum increases in intracellular $Ca^{2+}$ $[Ca^{2+}]_i$ evoked by 100 $\mu$M ATP. Data represent the mean ± S.E. of readings from three to five wells per cell line from four independent experiments (***, $p < 0.001$; *N.S.*, $p > 0.05$; one-way ANOVA). The *dashed line* represents the basal 340/380 ratio level. *C,* ATP-mediated dose-response curves for calcium flux in hHAP2Y$_2$R 1321N1 and hHAP2Y$_2$R cav1-KD 1321N1 cells were obtained using the Michaelis-Menten equation using GrahPad Prism ("Experimental Procedures"). Each data point represents the mean ± S.E. from three to four independent experiments, the pharmacodynamic parameters corresponding to each independent experiment were subsequently analyzed using an unpaired Student's *t* test (***, $p < 0.001$; *N.S.*, $p > 0.05$) (Table 1).

**TABLE 1**

**Summary of pharmacodynamic parameters for nucleotide-mediated dose response curves for calcium flux in hHAP2Y$_2$R 1321N1, hHAP2Y$_2$R cav1-KD 1321N1, wild type C6 controls, and C6 cav1-KD cells (see Figs. 5*C* and 6*D*)**

| | 1321N1 Astrocytoma Cells | | |
|---|---|---|---|
| Agonist = ATP | hHAP2Y$_2$R | hHAP2Y$_2$R cav1-KD | *p* value |
| $EC_{50}$ (nM) | 86.35 (± 2.49) | 77.16 (± 4.12) | 0.129 |
| Intrinsic activity ($\alpha$) | 1.0 (± 0.009) | 0.15 (± 0.002) | <0.0001 |
| | C6 glioma Cells | | |
| Agonist = UTP | C6 WT control | C6 cav1-KD | *p* value |
| $EC_{50}$ (μM) | 5.53 (± 0.39) | 7.86 (± 0.66) | 0.0397 |
| Intrinsic activity ($\alpha$) | 1.0 (± 0.02) | 0.21 (± 0.008) | <0.0001 |

or SCRAM shRNA-treated hHAP2Y$_2$ 1321N1 cells or WT 1321N1 cells (Fig. 2*B*; $n = 3$; ***, $p < 0.001$). Also, hHAP2Y$_2$R expression levels were not affected by treatment with the lentiviral particles, as determined by Western blot analysis (Fig. 2*A*, *upper panel*). Detergent-free sucrose gradient density fractionation of hHAP2Y$_2$R 1321 cells with shRNA-reduced Cav-1 expression levels caused a marked shift in the hHAP2Y$_2$R population to the high density, non-buoyant fractions 8–12 (Fig. 2*C*). A similar Cav-1 dependence of hHAP2Y$_2$R localization in membrane raft microdomains was further demonstrated using the microglia cell line BV-2 (53), which does not express Cav-1 (Fig. 1*D*). These results suggest that hHAP2Y$_2$R distribution in the raft compartment is Cav-1 dependent, as Flot-2-containing MRs were still detected even with the reduced or absence of Cav-1 expression. Subcellular fractionation assays using C6 glioma cells further demonstrate the residence of its endogenously expressed P2Y$_2$R in Cav-1 positive MRs and its dependence on agonist stimulation (Fig. 3). In addition, to provide additional evidence of the interaction between Cav-1 and P2Y$_2$R, Fig. 4 demonstrates the co-immunoprecipitation of these two proteins in C6 rat glioma cells (Fig. 4*A*) and PCRA (Fig. 4*B*). Even more, double transfection of HEK-293 cells, which have negligible Cav-1 and P2Y$_2$ levels (54–56), with FLAG-P2Y$_2$R and Cav-1-myc also permitted their co-immunoprecipitation (Fig. 4*C*).

*Knockdown of Cav-1 Expression Inhibits P2Y$_2$R-mediated Increases in $[Ca^{2+}]_i$*—Activation of the P2Y$_2$R stimulates phospholipase C and the generation of inositol 1,4,5-trisphosphate that induces the release of calcium from intracellular storage sites (44, 57). Therefore, we evaluated the effect of Cav-1 knockdown on P2Y$_2$R-mediated increases in $[Ca^{2+}]_i$ induced by 100 $\mu$M ATP. The ATP-induced increase in $[Ca^{2+}]_i$ was significantly reduced in hHAP2Y$_2$R 1321N1 cells after Cav-1 KD, as compared with uninfected cells or cells infected with SCRAM shRNA (Fig. 5*A*). Peak increases in $[Ca^{2+}]_i$ induced by 100 $\mu$M ATP were decreased after Cav-1 KD, as compared with uninfected or SCRAM shRNA-infected cells in a statistically significant manner (Fig. 5*B*) (***, $p < 0.001$). The dose-response curves obtained for the hHAP2Y$_2$R in 1321N1 cells revealed no significant differences in the $EC_{50}$ value for ATP (Fig. 5*C*, Table 1), whereas a highly statistically significant decrease (~85% reduction) in the intrinsic activity or maximal responses to ATP was seen in Cav-1 knockdown cells.

Rat C6 glioma cells express endogenously both Cav-1 and a repertoire of P2Y receptors, P2Y$_2$R included (26, 58, 59), which can be activated by UTP. The abolishment or reduction of P2Y$_2$R-mediated increases in $[Ca^{2+}]_i$ by shRNA Cav-1 knock-

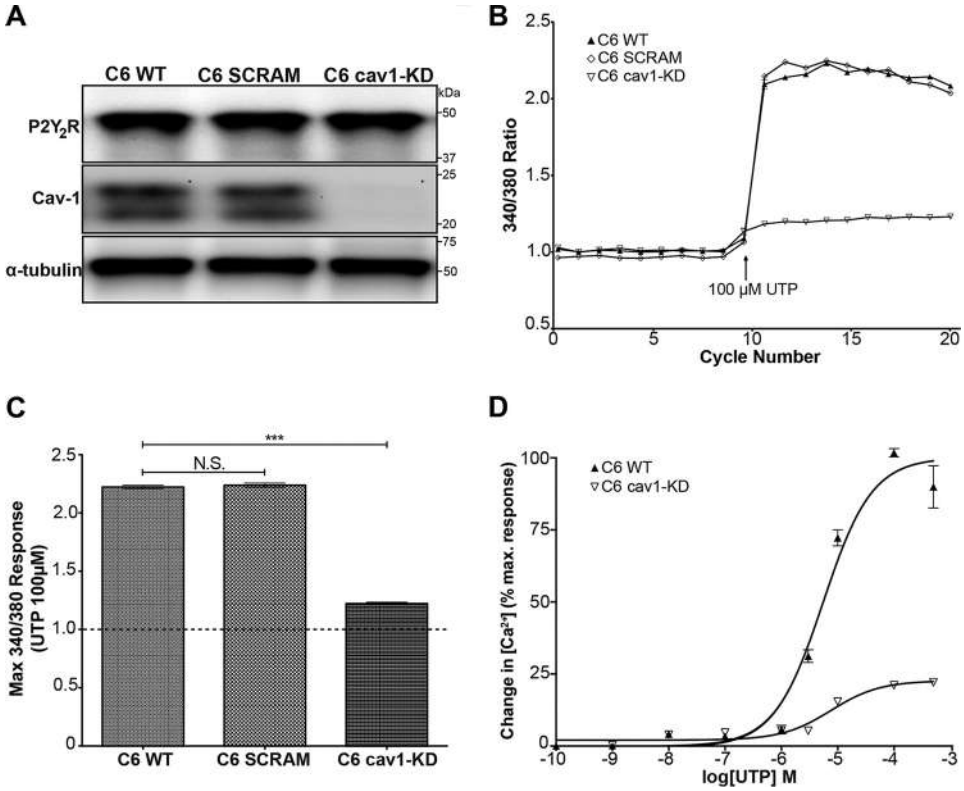


FIGURE 6. **Caveolin-1 knockdown inhibits P2Y$_2$R-mediated increases in $[Ca^{2+}]_i$ in C6 glioma cells.** *A,* representative immunoblot of P2Y$_2$R, Cav-1, and GAPDH (control) expression in WT C6 cells (*1st lane*), C6 cells after infection with scrambled (SCRAM) shRNA (*2nd lane*) or cav1 shRNA (*3rd lane*; cav1-KD) lentiviral particles. *B,* representative traces of intracellular calcium responses to 100 $\mu$M UTP in serum-starved WT C6 cells, C6 cav1-KD cells, and C6 cells infected with scrambled shRNA ($n = 5$). *C,* maximum increases in intracellular $Ca^{2+}$ $[Ca^{2+}]_i$ evoked by 100 $\mu$M UTP in WT C6, C6 SCRAM, and C6 cav1-KD cells. Data represent the mean ± S.E. of readings from three to five wells per cell line from four independent experiments where (***, $p < 0.001$; *N.S.*, $p > 0.05$; one-way ANOVA). The *dashed line* represents the basal 340/380 ratio level. *D,* UTP-mediated dose-response curves for calcium flux in hHAP2Y$_2$R 1321N1 and hHAP2Y$_2$R cav1-KD 1321N1 cells were obtained using the Michaelis-Menten equation using GraphPad Prism ("Experimental Procedures"). Each data point represents the mean ± S.E. from three to four independent experiments, the pharmacodynamic parameters corresponding to each independent experiment were subsequently analyzed using an unpaired Student's *t* test (***, $p < 0.001$; *N.S.*, $p > 0.05$) (Table 1).

down was further demonstrated in C6 glioma cells using 100 $\mu$M UTP (Fig. 6, *B* and *C*). Dose-response curves obtained for P2Y$_2$R in C6 cells revealed a slight but significant change in $EC_{50}$ value for UTP (Fig. 6*D*, Table 1), with the most statistically significant change also being a decrease (~79% reduction) in the maximal responses or intrinsic activity of UTP in Cav-1 knockdown cells.

The inhibition of P2Y$_2$R-mediated increases in $[Ca^{2+}]_i$ by knockdown of Cav-1 expression in 1321N1 cells seems to be largely selective, because it did not affect increases in $[Ca^{2+}]_i$ elicited by ionomycin, the PAR-1 receptor agonist TRAP-6 and carbachol (Fig. 7*A*). Similarly, no alteration by Cav-1 knockdown in C6 was seen for responses elicited by ionomycin and TRAP-6, because C6 do not mobilize $[Ca^{2+}]_i$ in response to carbachol (60) (Fig. 7*B*). The ionomycin results are also consistent with the fact that P2Y$_2$R mediated $Ca^{2+}$ signaling depends on the mobilization of intracellular $Ca^{2+}$ stores, and not on its entry.

*Knockdown of Cav-1 Inhibits P2Y$_2$R-mediated Akt Phosphorylation*—P2Y$_2$R activation leads to Akt phosphorylation in astrocytes (3, 10, 33), and other cell types (61, 62). In addition, Akt phosphorylation has been reported to be regulated by Cav-1 (63–65). Therefore, we examined the effect of Cav-1 KD in hHAP2Y$_2$R 1321N1 cells on ATP-induced Akt phosphorylation. Incubation of hHAP2Y$_2$R 1321N1 cells with 100 $\mu$M ATP increased Akt phosphorylation at Ser$^{473}$ within 10 min and Akt phosphorylation was maintained for more than 30 min (Fig. 8*A*). Cav-1 KD in hHAP2Y$_2$R 1321N1 cells significantly inhibited Akt phosphorylation at Ser$^{473}$ in response to 100 $\mu$M ATP regardless of time of exposure, whereas total Akt levels were unaffected (Fig. 8*B*). Densitometric analysis showed that Akt phosphorylation at Ser$^{473}$ induced by 100 $\mu$M ATP in hHAP2Y$_2$R 1321N1 cells was reduced after Cav-1 KD by ~50 and ~75% at 15 and 30 min, respectively, as compared with uninfected hHAP2Y$_2$R 1321N1 cells incubated with ATP (Fig. 8*C*).

*Cav-1 KD Fails to Sustain P2Y$_2$R-mediated ERK1/2 Phosphorylation*—P2Y$_2$R activation (10, 33, 37, 38) and Cav-1 expression (28, 66) are required for ERK1/2 phosphorylation in a variety of cell types. Thus, we examined whether Cav-1 KD inhibited ATP-induced ERK1/2 phosphorylation at Thr$^{202}$/Tyr$^{204}$ in hHAP2Y$_2$R 1321N1. As compared with ERK1/2 phosphorylation in response to 100 $\mu$M ATP in uninfected cells (Fig. 9*A*) Cav-1 KD in hHAP2Y$_2$R 1321N1 cells (Fig. 9*B*) were unable to sustain ERK1/2 phosphorylation at 30 min of ATP incubation. Total ERK1/2 levels were unaffected by Cav-1 KD. Densitometric analysis showed that ERK1/2 phosphorylation on Thr$^{202}$/Tyr$^{204}$ induced by 100 $\mu$M ATP in hHAP2Y$_2$R 1321N1 cells was significantly reduced by ~70% with Cav-1 KD

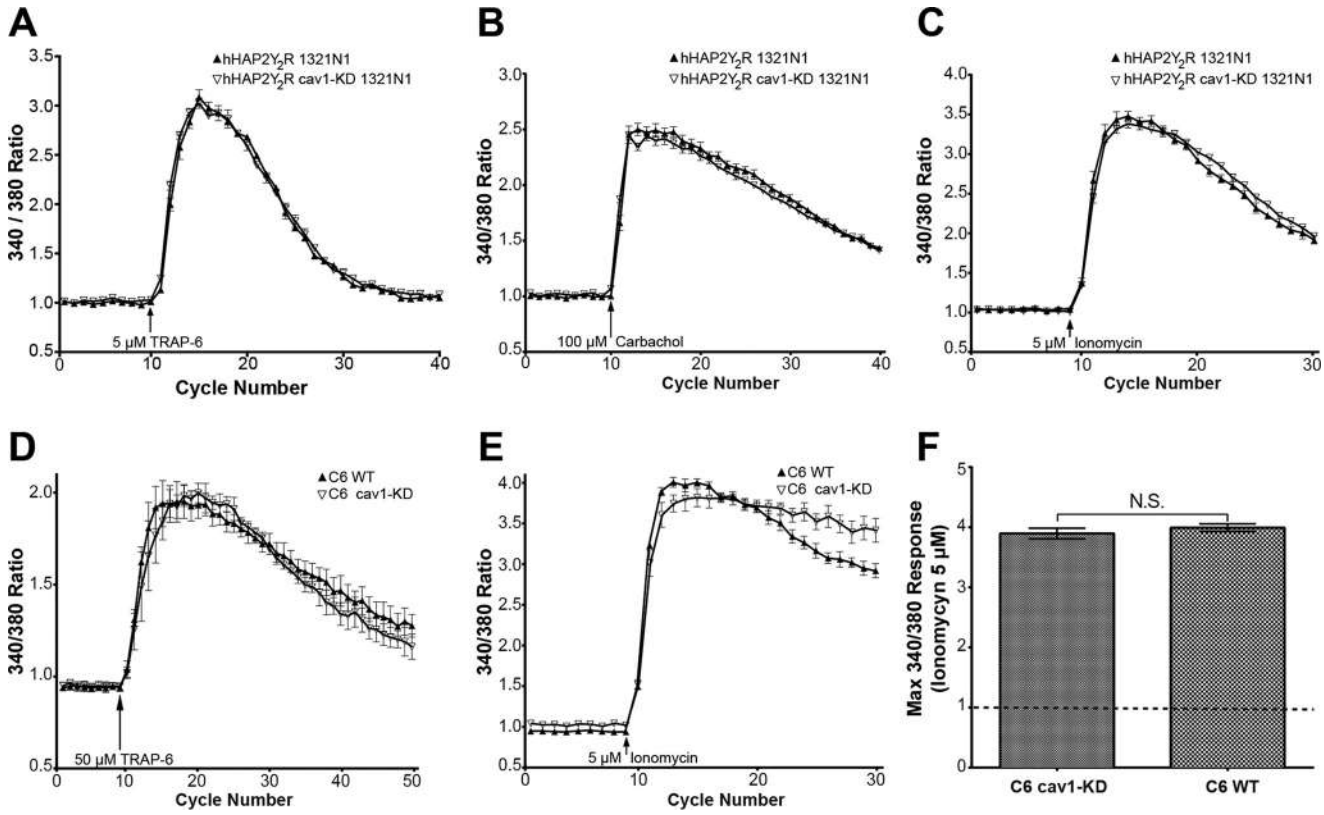


FIGURE 7. **Knockdown of Cav-1 expression impairs P2Y$_2$ receptor signaling without altering the signaling of other G$_q$-coupled receptors.** For these experiments hHAP2Y$_2$R 1321N1 cells, hHAP2Y$_2$R cav1-KD 1321N1 cells, WT C6, and shRNA-mediated cav1-KD glioma cells were plated onto 96-well plates, serum-starved for at least 16 h, and then exposed to the different agonists. Traces of intracellular calcium flux responses to (*A*) 5 $\mu$M TRAP-6, (*B*) 100 $\mu$M carbachol, and (*C*) 5 $\mu$M ionomycin in hHAP2Y$_2$R 1321N1 and hHAP2Y$_2$R cav1-KD 1321N1 cells; and traces of intracellular calcium flux responses to (*D*) 50 $\mu$M TRAP-6 and (*E*) 5 $\mu$M ionomycin in WT C6 and C6 cav1-KD cells. Data represent the mean ± S.E. of readings from three to five wells per cell line from four independent experiments. *F*, bar graph representing the maximal response of WT and cav1-KD C6 cells to the calcium ionophore ionomycin.

at 30 min, as compared with uninfected hHAP2Y$_2$R 1321N1 cells incubated with ATP (Fig. 9*C*).

## Discussion

The multipronged approach of this study revealed a dynamic and physiologically relevant interaction between the P2Y$_2$R and Cav-1 in human 1321N1 astrocytoma cells. The results were further validated using non-transfected glial cell lines endogenously expressing or devoid of P2Y$_2$R and/or Cav-1 (Figs. 2–7), and, HEK-293 cells doubly transfected with FLAG-P2Y$_2$R and Cav-1-myc, because these cells express extremely low levels of P2Y$_2$R and negligible levels of caveolin-1 (54–56) (Fig. 4*C*).

On the first hand, P2Y$_2$R were found to co-fractionate with Cav-1-rich MR fractions of 1321N1 cells (Fig. 1). Its localization in MRs was agonist (ATP) dependent, as agonist stimulation led to the migration of the receptor into higher density membrane fractions (Fig. 1). Similar experiments conducted in rat C6 glioma cells also demonstrate that P2Y$_2$R resides in MRs in an agonist-sensitive and -dependent manner (Fig. 3). The P2Y$_2$R/Cav-1 interaction and its sensitivity to agonist stimulation was demonstrated via co-immunoprecipitation assays (Fig. 1). Correspondingly, confocal microscopy revealed that both molecules co-localize in Cav-1 positive membrane microdomains of 1321N1 cells, and co-localization was diminished upon ATP stimulation (Fig. 1).

Furthermore, localization of the P2Y$_2$R in MRs was found to be dependent on Cav-1 expression, because knockdown of its expression (without alteration in the distribution of the raft marker protein flotillin-2) led to the migration of P2Y$_2$R into higher density membrane fractions. Use of BV-2 cells, a Cav-1 devoid microglial cell line expressing P2Y$_2$Rs, substantiates this finding, because P2Y$_2$R was found to reside in high density membrane fractions (Fig. 2) (67).

C6 cells and PCRA express endogenously both P2Y$_2$R and Cav-1, and co-immunoprecipitation assays further corroborated and determined the extent of the P2Y$_2$R/Cav-1 interaction in these glial cell model systems (Fig. 4). In turn, HEK-293 cells, which are basically devoid of P2Y$_2$R and caveolin-1 (54–56), were doubly transfected with FLAG-P2Y$_2$R and Cav-1-myc to further demonstrate their interaction via co-immunoprecipitation (Fig. 4*C*). Together, all of the above findings combined provide strong evidence on the interaction between the P2Y$_2$R and Cav-1.

It is important to note that receptor trafficking and signaling could be dependent on cell type (68, 69) and ligand specificity, leading to the activation of several caveolar and non-caveolar endocytic pathways (38, 70). In the case of the P2Y$_2$R, bioinformatic analysis further supports the molecular basis for its interaction with Cav-1 and caveolar MR residence. Analysis of the protein sequence of the human P2Y$_2$R (UniProt number P41231) reveals consensus sequences commonly regarded as caveolin-binding motifs (CBM: Ø*X*Ø*XXXX*Ø or Ø*XXXX*Ø*XX*Ø) (where Ø signifies F, W, or Y and, *X* signifies any amino acid) (71, 72). For example, two of the several canon-

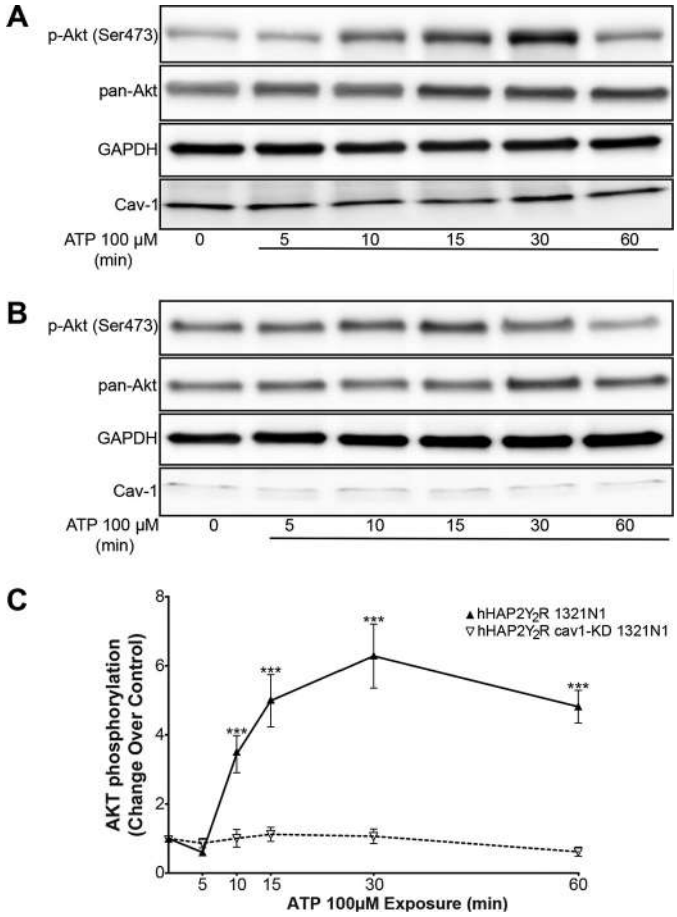


FIGURE 8. **Cav-1 is necessary for the P2Y$_2$R-mediated Akt phosphorylation.** *A* and *B*, hHAP2Y$_2$R 1321N1 cells were uninfected (*A*) or infected (*B*) with Cav-1 shRNA lentiviral particles, serum-starved for 16–24 h, and stimulated with 100 $\mu$M ATP in DMEM at 37 °C for 5, 10, 15, 30, and 60 min. DMEM only treated cells served as controls. Cells were lysed and Akt phosphorylation on Ser$^{473}$ and total Akt, Cav-1, and GAPDH (control) expression in equal amounts of protein were determined by Western blot analysis. Immunoblots are representative of at least three independent experiments. *C*, Akt phosphorylation on Ser$^{473}$ was normalized to total Akt levels and expressed as a percentage of untreated controls at 0 min. Values represent the mean ± S.E. ($n = 4$), where ***, $p < 0.001$ (one-way ANOVA) represent significant differences from ATP-treated cells to basal levels.

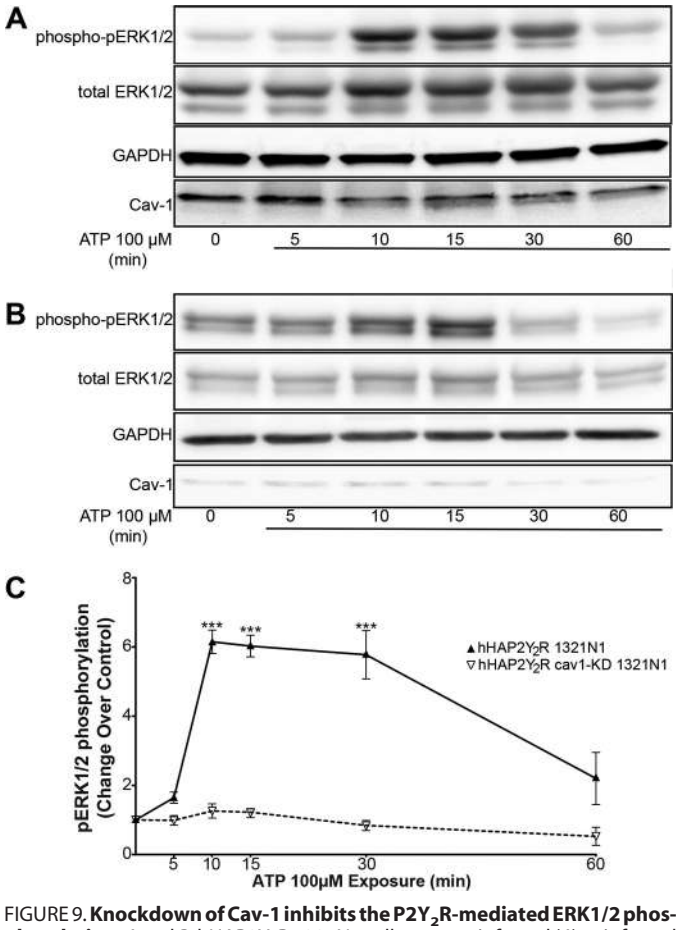


FIGURE 9. **Knockdown of Cav-1 inhibits the P2Y$_2$R-mediated ERK1/2 phosphorylation.** *A* and *B*, hHAP2Y$_2$R 1321N1 cells were uninfected (*A*) or infected (*B*) with Cav-1 shRNA lentiviral particles, then serum-starved for 16–24 h and stimulated with 100 $\mu$M ATP in DMEM at 37 °C for 5, 10, 15, 30, and 60 min. DMEM only treated cells served as controls. Cells were lysed and ERK1/2 phosphorylation on Thr$^{202}$/Tyr$^{204}$ and expression of total ERK1/2, Cav-1, and GAPDH (control) in equal amounts of protein were determined by Western blotting analysis. Immunoblots are representative of three independent experiments. *C*, ERK1/2 phosphorylation on Thr$^{202}$/Tyr$^{204}$ was normalized to total ERK1/2 levels and expressed as a percentage of untreated controls at 0 min. Values represent the mean ± S.E. ($n = 4$), where ***, $p < 0.001$ (one-way ANOVA) represent significant differences from ATP-treated cells to basal levels.

ical CBM found within the human P2Y$_2$R protein sequence rest arranged within amino acids 56 to 65, and 65 to 73. Interestingly, these domains are evolutionarily conserved in human, mouse, and rat P2Y$_2$R protein sequences. These motifs may operate as a "molecular control switch" that regulates P2Y$_2$R trafficking (16, 73–75). Future P2Y$_2$R mutagenesis experiments should evaluate whether the CBMs in the P2Y$_2$R regulate Cav-1-dependent P2Y$_2$R trafficking from MRs and whether other protein interactions are involved. Nevertheless, it is clear that P2Y$_2$R localization and interaction with Cav-1-positive in caveolar MR microdomains is a dynamic process required for optimal receptor function.

It is noteworthy that a previous study (36) done in HEK-293 cells did not consider the fact that these cells express extremely low to negligible levels of caveolin-1 and are considered to be caveolin-1 devoid (54). Consequently, the role of caveolin-1 in P2Y$_2$R endocytic behaviors cannot be accurately determined in the naive HEK-293 model system. An additional, weakened aspect of the latter study was the use of methyl-$\beta$-cyclodextrin (a typical inhibitor of caveolar endocytosis) to "block clathrin-mediated endocytosis," among others. Hence the value and appropriateness of the Cav-1-KD models developed and analyzed in our study to accurately determine the caveolar MR residence of the P2Y$_2$R and the modulatory role of Cav-1 of its signaling pathways in 1321N1 cells.

To establish the physiological relevance of the interaction between Cav-1 and P2Y$_2$R, the impact of Cav-1 knockdown in P2Y$_2$R-mediated signaling in 1321N1 cells was assessed. Consequently, P2Y$_2$R-mediated increases in $[Ca^{2+}]_i$ mobilization was significantly reduced by silencing Cav-1 expression in both 1321N1 (Fig. 5) and C6 cells (Fig. 6). Hence, P2Y$_2$R interaction with Cav-1 in plasma MRs is required for nucleotide agonists to induce maximal intracellular calcium mobilization. Indeed, the agonist-mediated P2Y$_2$R receptor $Ca^{2+}$ mobilization in undifferentiated C6 cells is blocked by the caveolar membrane raft disrupting agent methyl-$\beta$-cyclodextrin, and, upon differentiation of these cells, down-regulation of the P2Y$_2$ receptor

is observed with abolishment of the UTP-mediated $Ca^{2+}$ responses.[4]

The reduction in P2Y$_2$R-mediated increases in $[Ca^{2+}]_i$ was both time and agonist concentration dependent, as evidenced by the kinetics and dose-response curves for ATP and UTP, in 1321N1 and C6 cells, respectively. The reduction by Cav-1 knockdown of P2Y$_2$R-mediated changes in $[Ca^{2+}]_i$ seems to be selective, because the increases in intracellular $[Ca^{2+}]_i$ elicited by the muscarinic agonist carbachol and TRAP-6 were unaffected in 1321N1 cells (Fig. 7). Similarly, in C6 cells (which lack muscarinic receptors) the PAR-1 receptor agonist TRAP-6 $[Ca^{2+}]_i$ responses were unaffected by Cav-1 knockdown. In both cell types, the ionophore ionomycin $[Ca^{2+}]_i$ responses were also not altered by knockdown of Cav-1 (Fig. 7).

Herein, it is clearly established that silencing caveolin-1 expression significantly and selectively reduced P2Y$_2$R-dependent increases in $[Ca^{2+}]_i$ in hHAP2Y$_2$R 1321N1 cells and C6 cells by ~80–85% after Cav-1 KD, as compared with their respective Cav-1 controls. The remaining calcium responses seen may relate to the remaining Cav-1 in these cells or additional Cav-1-independent mechanisms that can also induce P2Y$_2$R-mediated calcium mobilization. Similar reductions in P2Y receptor-dependent increases in $[Ca^{2+}]_i$ have been reported with suppression of Cav-1 expression in C6 glial cells (40). Furthermore, P2Y$_2$R interaction with Cav-1 in plasma MRs is required for ATP to induce Akt and ERK1/2 phosphorylation (Figs. 8 and 9), as demonstrated by statistically significant reductions in Cav-1 KD hHAP2Y$_2$ 1321N1 cells.

Stimulation of the P2Y$_2$R with ATP and Cav-1 KD in hHAP2Y$_2$R 1321N1 cells leads to a redistribution of the P2Y$_2$R to a high-density membrane domain that does not contain Flot-2 or Cav-1; hence, strongly suggesting that ATP can induce Cav-1 dissociation from the P2Y$_2$R thereby releasing the receptor from plasma MRs and/or associated signaling complexes (Fig. 10). The P2Y$_2$R and Cav-1 co-exist in a well organized MR complex under basal conditions, whereas ligand binding appears to elicit activation of its signaling pathways, concomitant with redistribution of the P2Y$_2$R into non-caveolar MRs microdomains (Fig. 10). Kinetic studies must be done to precisely determine whether Cav-1 interacts with the P2Y$_2$R permitting its compartmentalization in CAV with its signaling machinery, yet in an "inactive receptor" state promoted by Cav-1. Agonist stimulation may hence lead to its dissociation from Cav-1 promoting an "active receptor" state, which permits its coupling to its signaling pathway effectors, and subsequently migrate into non-raft microdomains in a "desensitized" or "uncoupled" receptor state. Thus, the P2Y$_2$R may be fully active when located in caveolar MRs, although not necessarily bound to Cav-1, and, calcium mobilization and Akt and ERK1/2 phosphorylation are decreased when the receptor is redistributed out of these Cav-1 positive rafts. Alternatively, initial spatiotemporal calcium signaling events may take place in the caveolar raft microdomains, whereas subsequent Akt and ERK1/2 activation take place in non-caveolar raft microdomains such as clathrin-coated pits/vesicles and endosomes (76, 77). This

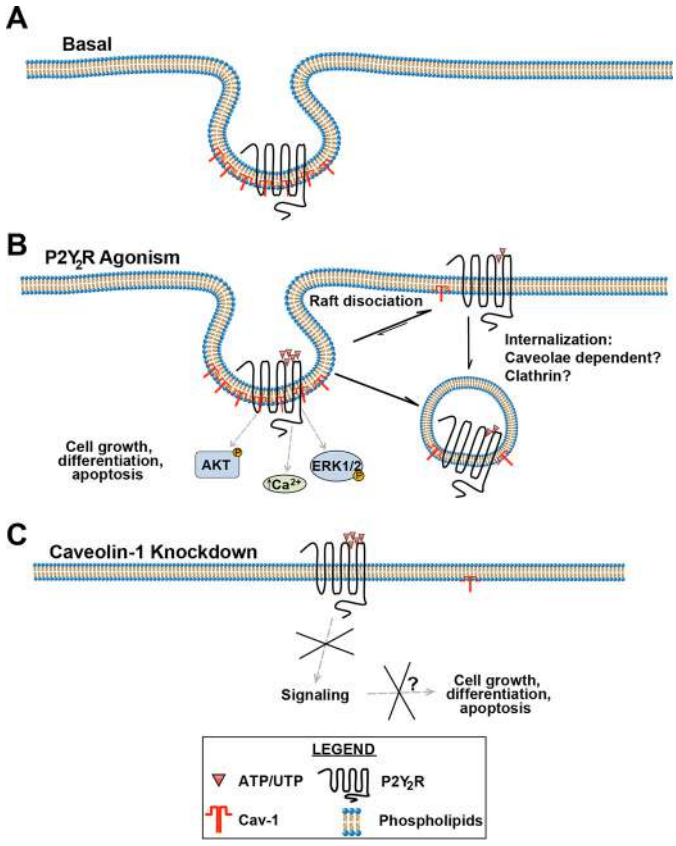


FIGURE 10. **Caveolin-1 modulates P2Y$_2$R signaling in 1321N1 cells.** A schematic representation describing the Cav-1-dependent P2Y$_2$R-mediated signaling pathways investigated in this study. *A,* basal state P2Y$_2$R localization in caveolar membrane raft microdomains is mediated by its interaction with caveolin-1. *B,* nucleotide agonists activation of the P2Y$_2$R signaling pathways, subsequent dissociation from caveolin-1 with migration into non-caveolar raft microdomains. *C,* caveolin-1 knockdown or absence leads to P2Y$_2$R expression in non-caveolar membrane raft microdomains and uncoupling from its signaling pathways.

behavior is reminiscent of possible P2Y$_2$R desensitization or uncoupling as previously observed (44, 57), and may correlate with the proposed clathrin-mediated endocytosis of the receptor seen in HEK-293 cells (36). The spatial distribution of the receptor between caveolar and non-caveolar subcellular compartments may modulate the temporal signaling responses duration and magnitudes by concerting the location of intracellular second messenger production relative to effectors (77). It has also been suggested that MRs at the cellular surface may be involved in the regulation of receptor stability (78). Therefore, P2Y$_2$Rs located in the MRs may become more resistant to rapid internalization, thus allowing it to couple to specific signaling pathways. This venue, however, remains to be explored. Most importantly, our findings are consistent with other studies that have made compelling arguments regarding the existence of purinergic receptors in caveolae consequently providing an enriched environment for integrating necessary interactions for signal transduction (39, 79, 80).

Regarding the exact mechanisms by which caveolin-1 regulates P2Y$_2$R-mediated Akt and ERK1/2 phosphorylation remain to be elucidated. β-Arrestins have been suggested to regulate the activation of MAPKs and Akt by G protein-coupled receptors by inducing receptor endocytosis and relocaliza-

[4] N. A. Martinez, A. M. Ayala, M. Martinez, F. J. Martinez-Rivera, J. D. Miranda, and W. I. Silva, unpublished results.

tion to intracellular structures (70, 76, 81, 82). Indeed, a previous study suggested a role for clathrin-mediated endocytosis in P2Y$_2$R trafficking (36). Activation of the P2Y$_2$R by ATP has been shown to promote interaction with β-arrestin-1, which alters the duration of ERK1/2 activation (38), similar to the effect of ATP and Cav-1 KD on P2Y$_2$R-mediated ERK1/2 activation in the current study. The duration of ERK1/2 activation has been found to determine cell fate (83) and Cav-1 has been reported to enhance the interaction between β-arrestin-2 and the neurokinin-1 receptor to regulate clathrin-mediated receptor endocytosis and signaling (84). It is tempting to speculate that Cav-1 might also affect the behavior of β-arrestin-1 upon P2Y$_2$R activation in hHAP2Y$_2$R 1321N1 cells. Moreover, dephosphorylation of Akt is catalyzed by protein phosphatases PP1 and PP2A (85–87), which might represent a key regulation point of Cav-1, previously shown to negatively modulate their activity (64). Clearly, the precise mechanisms by which Cav-1 modulates P2Y$_2$R-mediated Akt and ERK1/2 phosphorylation remains to be determined, considering other subcellular compartments (32).

To date, only a few studies have investigated the role of caveolin-1 in the regulation of P2Y$_2$R signaling (36, 39, 41, 67, 88), although these studies have provided limited or conflicting information on this pathway. The current study conclusively demonstrates that the P2Y$_2$R is a caveolar MR resident protein and its interaction with Cav-1 modulates the signaling responses to P2Y$_2$R nucleotide agonists. These findings may unveil promising targets for drug discovery and the development of treatment for conditions where both molecules have been shown to play a role, such as in neurodegenerative diseases, cancer, and brain injury (8, 89–93).

*Author Contributions*—N. A. M. and W. I. S. conceived and designed the study. N. A. M., A. M. A., and M. M. performed the discontinuous sucrose density gradient fractionations, signaling and calcium mobilization experiments, designed and purified the plasmids, shRNA cav-1 knockdown, and cultivated and treated cells. N. A. M. and F. J. M. performed the immunoprecipitation experiments. N. A. M., A. M. A., M. M., F. J. M., J. D. M., and W. I. S. analyzed data and interpreted results of experiments; N. A. M. and W. I. S. prepared the figures. N. A. M. and W. I. S. drafted the manuscript. N. A. M., A. M. A., M. M., F. J. M., J. D. M., and W. I. S. edited, revised, and approved the final version of manuscript.

*Acknowledgments—We thank Dr. G. A. Weisman for kindly providing the WT 1321N1, pLXSN 1321N1, and hHAP2Y$_2$R 1321N1 astrocytoma cells; Dr. Jeffrey E. Pessin for kindly providing the Myc-tagged human caveolin-1 pcDNA3.1 expression vector; Dr. Priscila Sanabria (Universidad Central del Caribe, PR) for support with the calcium flux and confocal microscopy imaging studies. We also thank Mónica Quiñones for support in some of the experiments. Some of the experiments were performed at the RCMI Facilities of the University of Puerto Rico, MSC, and Universidad Central del Caribe. Shared instrumentation was supported by NCRR Grants G12RR003051 and G12RR03035, at the UPR-MSC and Universidad Central del Caribe, respectively. The Confocal Microscopy Facility at UPR-RP was supported by Grants ISI0 RR-13705-01 and DBI-0923132. Some experiments were performed at the Molecular Sciences Research Building of the University of Puerto Rico.*

**References**


1. Duncan, G. W. (2011) The aging brain and neurodegenerative diseases. *Clin. Geriatr. Med.* **27,** 629–644
2. Yankner, B. A., Lu, T., and Loerch, P. (2008) The aging brain. *Annu. Rev. Pathol.* **3,** 41–66
3. Abbracchio, M. P., and Ceruti, S. (2006) Roles of P2 receptors in glial cells: focus on astrocytes. *Purinergic Signal.* **2,** 595–604
4. Lazarowski, E. R., Homolya, L., Boucher, R. C., and Harden, T. K. (1997) Direct demonstration of mechanically induced release of cellular UTP and its implication for uridine nucleotide receptor activation. *J. Biol. Chem.* **272,** 24348–24354
5. Luttikhuizen, D. T., Harmsen, M. C., de Leij, L. F., and van Luyn, M. J. (2004) Expression of P2 receptors at sites of chronic inflammation. *Cell Tissue Res.* **317,** 289–298
6. Miras-Portugal, M. T., Diaz-Hernandez, J. I., Gomez-Villafuertes, R., Diaz-Hernandez, M., Artalejo, A. R., and Gualix, J. (2015) Role of P2X7 and P2Y2 receptors on α-secretase-dependent APP processing: control of amyloid plaques formation "*in vivo*" by P2X7 receptor. *Comput. Struct. Biotechnol. J.* **13,** 176–181
7. Peterson, T. S., Camden, J. M., Wang, Y., Seye, C. I., Wood, W. G., Sun, G. Y., Erb, L., Petris, M. J., and Weisman, G. A. (2010) P2Y2 nucleotide receptor-mediated responses in brain cells. *Mol. Neurobiol.* **41,** 356–366
8. Peterson, T. S., Thebeau, C. N., Ajit, D., Camden, J. M., Woods, L. T., Wood, W. G., Petris, M. J., Sun, G. Y., Erb, L., and Weisman, G. A. (2013) Up-regulation and activation of the P2Y2 nucleotide receptor mediate neurite extension in IL-1β-treated mouse primary cortical neurons. *J. Neurochem.* **125,** 885–896
9. Arthur, D. B., Akassoglou, K., and Insel, P. A. (2005) P2Y2 receptor activates nerve growth factor/TrkA signaling to enhance neuronal differentiation. *Proc. Natl. Acad. Sci. U.S.A.* **102,** 19138–19143
10. Arthur, D. B., Georgi, S., Akassoglou, K., and Insel, P. A. (2006) Inhibition of apoptosis by P2Y2 receptor activation: novel pathways for neuronal survival. *J. Neurosci.* **26,** 3798–3804
11. Arthur, D. B., Taupenot, L., and Insel, P. A. (2007) Nerve growth factor-stimulated neuronal differentiation induces changes in P2 receptor expression and nucleotide-stimulated catecholamine release. *J. Neurochem.* **100,** 1257–1264
12. Kong, Q., Peterson, T. S., Baker, O., Stanley, E., Camden, J., Seye, C. I., Erb, L., Simonyi, A., Wood, W. G., Sun, G. Y., and Weisman, G. A. (2009) Interleukin-1beta enhances nucleotide-induced and α-secretase-dependent amyloid precursor protein processing in rat primary cortical neurons via up-regulation of the P2Y2 receptor. *J. Neurochem.* **109,** 1300–1310
13. Li, H.-J., Wang, L.-Y., Qu, H.-N., Yu, L.-H., Burnstock, G., Ni, X., Xu, M., and Ma, B. (2011) P2Y2 receptor-mediated modulation of estrogen-induced proliferation of breast cancer cells. *Mol. Cell. Endocrinol.* **338,** 28–37
14. Tran, M. D. (2011) P2 receptor stimulation induces amyloid precursor protein production and secretion in rat cortical astrocytes. *Neurosci. Lett.* **492,** 155–159
15. Rodríguez-Zayas, A. E., Torrado, A. I., and Miranda, J. D. (2010) P2Y2 receptor expression is altered in rats after spinal cord injury. *Int. J. Dev. Neurosci.* **28,** 413–421
16. Patel, H. H., Murray, F., and Insel, P. A. (2008) Caveolae as organizers of pharmacologically relevant signal transduction molecules. *Annu. Rev. Pharmacol. Toxicol.* **48,** 359–391
17. Patel, H. H., and Insel, P. A. (2009) Lipid rafts and caveolae and their role in compartmentation of redox signaling. *Antioxid. Redox Signal.* **11,** 1357–1372
18. Pani, B., and Singh, B. B. (2009) Lipid rafts/caveolae as microdomains of calcium signaling. *Cell Calcium* **45,** 625–633
19. Schroeder, F., Atshaves, B. P., Gallegos, A. M., McIntosh, A. L., Liu, J. C. S., Kier, A. B., Huang, H., and Ball, J. M. (2005) Lipid rafts and caveolae organization. In *Caveolae and Lipid Rafts: Roles in Signal Transduction and the Pathogenesis of Human Disease,* pp. 1–36, Advances in Molecular and Cell Biology, Elsevier, Amsterdam
20. Bittar, E. (2005) *Caveolae and Lipid Rafts: Roles in Signal Transduction and the Pathogenesis of Human Disease*, Elsevier Science Publishing Co.,

Inc., New York
21. Pike, L. J. (2006) Rafts defined: a report on the Keystone Symposium on Lipid Rafts and Cell Function. *J. Lipid Res.* **47,** 1597–1598
22. Okamoto, T., Schlegel, A., Scherer, P. E., and Lisanti, M. P. (1998) Caveolins, a family of scaffolding proteins for organizing "preassembled signaling complexes" at the plasma membrane. *J. Biol. Chem.* **273,** 5419–5422
23. Smart, E. J., Graf, G. A., McNiven, M. A., Sessa, W. C., Engelman, J. A., Scherer, P. E., Okamoto, T., and Lisanti, M. P. (1999) Caveolins, liquid-ordered domains, and signal transduction. *Mol. Cell. Biol.* **19,** 7289–7304
24. Chini, B., and Parenti, M. (2004) G-protein coupled receptors in lipid rafts and caveolae: how, when and why do they go there? *J. Mol. Endocrinol.* **32,** 325–338
25. Zhu, X. D., Zhuang, Y., Ben, J. J., Qian, L. L., Huang, H. P., Bai, H., Sha, J. H., He, Z. G., and Chen, Q. (2011) Caveolae-dependent endocytosis is required for class A macrophage scavenger receptor-mediated apoptosis in macrophages. *J. Biol. Chem.* **286,** 8231–8239
26. Silva, W. I., Maldonado, H. M., Velázquez, G., García, J. O., and González, F. A. (2007) Caveolins in glial cell model systems: from detection to significance. *J. Neurochem.* **103,** 101–112
27. Salgado, I. K., Serrano, M., García, J. O., Martínez, N. A., Maldonado, H. M., Báez-Pagán, C. A., Lasalde-Dominicci, J. A., and Silva, W. I. (2012) SorLA in glia: shared subcellular distribution patterns with caveolin-1. *Cell. Mol. Neurobiol.* **32,** 409–421
28. Head, B. P., Patel, H. H., Tsutsumi, Y. M., Hu, Y., Mejia, T., Mora, R. C., Insel, P. A., Roth, D. M., Drummond, J. C., and Patel, P. M. (2008) Caveolin-1 expression is essential for *N*-methyl-D-aspartate receptor-mediated Src and extracellular signal-regulated kinase 1/2 activation and protection of primary neurons from ischemic cell death. *FASEB J.* **22,** 828–840
29. Sato, M., Hutchinson, D. S., Halls, M. L., Furness, S. G., Bengtsson, T., Evans, B. A., and Summers, R. J. (2012) Interaction with caveolin-1 modulates G protein coupling of mouse $\beta$3-adrenoceptor. *J. Biol. Chem.* **287,** 20674–20688
30. Kong, M. M., Hasbi, A., Mattocks, M., Fan, T., O'Dowd, B. F., and George, S. R. (2007) Regulation of D1 dopamine receptor trafficking and signaling by caveolin-1. *Mol. Pharmacol.* **72,** 1157–1170
31. Meyer, C., Liu, Y., Kaul, A., Peipe, I., and Dooley, S. (2013) Caveolin-1 abrogates TGF-$\beta$ mediated hepatocyte apoptosis. *Cell Death Dis.* **4,** e466
32. Fridolfsson, H. N., Roth, D. M., Insel, P. A., and Patel, H. H. (2014) Regulation of intracellular signaling and function by caveolin. *FASEB J.* **28,** 3823–3831
33. Burgos, M., Neary, J. T., and González, F. A. (2007) P2Y2 nucleotide receptors inhibit trauma-induced death of astrocytic cells. *J. Neurochem.* **103,** 1785–1800
34. Chorna, N. E., Santiago-Pérez, L. I., Erb, L., Seye, C. I., Neary, J. T., Sun, G. Y., Weisman, G. A., and González, F. A. (2004) P2Y receptors activate neuroprotective mechanisms in astrocytic cells. *J. Neurochem.* **91,** 119–132
35. Neary, J. T., and Zimmermann, H. (2009) Trophic functions of nucleotides in the central nervous system. *Trends Neurosci.* **32,** 189–198
36. Tulapurkar, M. E., Schäfer, R., Hanck, T., Flores, R. V., Weisman, G. A., González, F. A., and Reiser, G. (2005) Endocytosis mechanism of P2Y2 nucleotide receptor tagged with green fluorescent protein: clathrin and actin cytoskeleton dependence. *Cell Mol. Life Sci.* **62,** 1388–1399
37. Morris, G. E., Nelson, C. P., Brighton, P. J., Standen, N. B., Challiss, R. A., and Willets, J. M. (2012) Arrestins 2 and 3 differentially regulate ETA and P2Y2 receptor-mediated cell signaling and migration in arterial smooth muscle. *Am. J. Physiol. Cell Physiol.* **302,** C723–C734
38. Hoffmann, C., Ziegler, N., Reiner, S., Krasel, C., and Lohse, M. J. (2008) Agonist-selective, receptor-specific interaction of human P2Y receptors with $\beta$-arrestin-1 and -2. *J. Biol. Chem.* **283,** 30933–30941
39. D' Ambrosi, N., and Volonte, C. (2013) Metabotropic purinergic receptors in lipid membrane microdomains. *Curr. Med. Chem.* **20,** 56–63
40. Bhatnagar, A., Sheffler, D. J., Kroeze, W. K., Compton-Toth, B., and Roth, B. L. (2004) Caveolin-1 interacts with 5-HT2A serotonin receptors and profoundly modulates the signaling of selected $G_q$-coupled protein receptors. *J. Biol. Chem.* **279,** 34614–34623
41. Ando, K., Obara, Y., Sugama, J., Kotani, A., Koike, N., Ohkubo, S., and Nakahata, N. (2010) P2Y2 receptor-Gq/11 signaling at lipid rafts is required for UTP-induced cell migration in NG 108–15 cells. *J. Pharmacol Exp. Ther.* **334,** 809–819
42. Nguyen, T., Erb, L., Weisman, G. A., Marchese, A., Heng, H. H., Garrad, R. C., George, S. R., Turner, J. T., and O'Dowd, B. F. (1995) Cloning, expression, and chromosomal localization of the human uridine nucleotide receptor gene. *J. Biol. Chem.* **270,** 30845–30848
43. Erb, L., Garrad, R., Wang, Y., Quinn, T., Turner, J. T., and Weisman, G. A. (1995) Site-directed mutagenesis of P2U purinoceptors: positively charged amino acids in transmembrane helices 6 and 7 affect agonist potency and specificity. *J. Biol. Chem.* **270,** 4185–4188
44. Flores, R. V., Hernández-Pérez, M. G., Aquino, E., Garrad, R. C., Weisman, G. A., and Gonzalez, F. A. (2005) Agonist-induced phosphorylation and desensitization of the P2Y2 nucleotide receptor. *Mol. Cell Biochem.* **280,** 35–45
45. Silva, W. I., Maldonado, H. M., Velázquez, G., Rubio-Dávila, M., Miranda, J. D., Aquino, E., Mayol, N., Cruz-Torres, A., Jardón, J., and Salgado-Villanueva, I. K. (2005) Caveolin isoform expression during differentiation of C6 glioma cells. *Int. J. Dev. Neurosci.* **23,** 599–612
46. Adami, C., Sorci, G., Blasi, E., Agneletti, A. L., Bistoni, F., and Donato, R. (2001) S100B expression in and effects on microglia. *Glia* **33,** 131–142
47. Silva, W. I., Maldonado, H. M., Lisanti, M. P., Devellis, J., Chompré, G., Mayol, N., Ortiz, M., Velázquez, G., Maldonado, A., and Montalvo, J. (1999) Identification of caveolae and caveolin in C6 glioma cells. *Int. J. Dev. Neurosci.* **17,** 705–714
48. Ho, S. N., Hunt, H. D., Horton, R. M., Pullen, J. K., and Pease, L. R. (1989) Site-directed mutagenesis by overlap extension using the polymerase chain reaction. *Gene* **77,** 51–59
49. Shigematsu, S., Watson, R. T., Khan, A. H., and Pessin, J. E. (2003) The adipocyte plasma membrane caveolin functional/structural organization is necessary for the efficient endocytosis of GLUT4. *J. Biol. Chem.* **278,** 10683–10690
50. Sromek, S. M., and Harden, T. K. (1998) Agonist-induced internalization of the P2Y2 receptor. *Mol. Pharmacol.* **54,** 485–494
51. Zinchuk, V., Wu, Y., Grossenbacher-Zinchuk, O., and Stefani, E. (2011) Quantifying spatial correlations of fluorescent markers using enhanced background reduction with protein proximity index and correlation coefficient estimations. *Nat. Protoc.* **6,** 1554–1567
52. Dunn, K. W., Kamocka, M. M., and McDonald, J. H. (2011) A practical guide to evaluating colocalization in biological microscopy. *Am. J. Physiol. Cell Physiol.* **300,** C723–C742
53. Rimmerman, N., Bradshaw, H. B., Kozela, E., Levy, R., Juknat, A., and Vogel, Z. (2012) Compartmentalization of endocannabinoids into lipid rafts in a microglial cell line devoid of caveolin-1. *Br. J. Pharmacol.* **165,** 2436–2449
54. Wang, L., Connelly, M. A., Ostermeyer, A. G., Chen, H.-H., Williams, D. L., and Brown, D. A. (2003) Caveolin-1 does not affect SR-BI-mediated cholesterol efflux or selective uptake of cholesteryl ester in two cell lines. *J. Lipid Res.* **44,** 807–815
55. Vöhringer, C., and Reiser, G. (2001) Pharmacological characterization of the rat brain P2Y1 receptor expressed in HEK293 cells: $Ca^{2+}$ signaling and receptor regulation. *Drug Dev. Res.* **53,** 172–179
56. Moskvina, E., Unterberger, U., and Boehm, S. (2003) Activity-dependent autocrine-paracrine activation of neuronal P2Y receptors. *J. Neurosci.* **23,** 7479–7488
57. Otero, M., Garrad, R. C., Velázquez, B., Hernández-Pérez, M. G., Camden, J. M., Erb, L., Clarke, L. L., Turner, J. T., Weisman, G. A., and González, F. A. (2000) Mechanisms of agonist-dependent and -independent desensitization of a recombinant P2Y2 nucleotide receptor. *Mol. Cell. Biochem.* **205,** 115–123
58. Wypych, D., and Barańska, J. (2013) Cross-talk in nucleotide signaling in glioma C6 cells. *Adv. Exp. Med. Biol.* **986,** 31–59
59. Wypych, D., and Pomorski, P. (2012) P2Y1 nucleotide receptor silencing and its effect on glioma C6 calcium signaling. *Acta Biochim. Pol.* **59,** 711–717
60. Singh, S. P., Gao, Y., Kunapuli, S. P., and Ravindra, R. (1998) Glucose uptake by C6 glioma cells is mediated by G(q$\alpha$). *Neuroreport* **9,** 115–119
61. Katz, S., Ayala, V., Santillán, G., and Boland, R. (2011) Activation of the PI3K/Akt signaling pathway through $P2Y_2$ receptors by extracellular ATP

is involved in osteoblastic cell proliferation. *Arch. Biochem. Biophys.* **513,** 144–152
62. Ding, L., Ma, W., Littmann, T., Camp, R., and Shen, J. (2011) The P2Y2 nucleotide receptor mediates tissue factor expression in human coronary artery endothelial cells. *J. Biol. Chem.* **286,** 27027–27038
63. Cordes, N., Frick, S., Brunner, T. B., Pilarsky, C., Grützmann, R., Sipos, B., Klöppel, G., McKenna, W. G., and Bernhard, E. J. (2007) Human pancreatic tumor cells are sensitized to ionizing radiation by knockdown of caveolin-1. *Oncogene.* **26,** 6851–6862
64. Li, L., Ren, C. H., Tahir, S. A., Ren, C., and Thompson, T. C. (2003) Caveolin-1 maintains activated Akt in prostate cancer cells through scaffolding domain binding site interactions with and inhibition of serine/threonine protein phosphatases PP1 and PP2A. *Mol. Cell. Biol.* **23,** 9389–9404
65. Gonzalez, E., Nagiel, A., Lin, A. J., Golan, D. E., and Michel, T. (2004) Small interfering RNA-mediated down-regulation of caveolin-1 differentially modulates signaling pathways in endothelial cells. *J. Biol. Chem.* **279,** 40659–40669
66. del Pozo, M. A., Balasubramanian, N., Alderson, N. B., Kiosses, W. B., Grande-García, A., Anderson, R. G., and Schwartz, M. A. (2005) Phosphocaveolin-1 mediates integrin-regulated membrane domain internalization. *Nat. Cell Biol.* **7,** 901–908
67. Norambuena, A., Palma, F., Poblete, M. I., Donoso, M. V., Pardo, E., González, A., and Huidobro-Toro, J. P. (2010) UTP controls cell surface distribution and vasomotor activity of the human P2Y2 receptor through an epidermal growth factor receptor-transregulated mechanism. *J. Biol. Chem.* **285,** 2940–2950
68. Mayor, S., and Pagano, R. E. (2007) Pathways of clathrin-independent endocytosis. *Nat. Rev. Mol. Cell Biol.* **8,** 603–612
69. Choudhury, A., Marks, D. L., Proctor, K. M., Gould, G. W., and Pagano, R. E. (2006) Regulation of caveolar endocytosis by syntaxin 6-dependent delivery of membrane components to the cell surface. *Nat. Cell Biol.* **8,** 317–328
70. DeWire, S. M., Ahn, S., Lefkowitz, R. J., and Shenoy, S. K. (2007) β-Arrestins and cell signaling. *Annu. Rev. Physiol.* **69,** 483–510
71. Couet, J., Li, S., Okamoto, T., Ikezu, T., and Lisanti, M. P. (1997) Identification of peptide and protein ligands for the caveolin-scaffolding domain: implications for the interaction of caveolin with caveolae-associated proteins. *J. Biol. Chem.* **272,** 6525–6533
72. Spisni, E., Tomasi, V., Cestaro, A., and Tosatto, S. C. (2005) Structural insights into the function of human caveolin 1. *Biochem. Biophys. Res. Commun.* **338,** 1383–1390
73. Ostrom, R. S. (2002) New determinants of receptor-effector coupling: trafficking and compartmentation in membrane microdomains. *Mol. Pharmacol.* **61,** 473–476
74. Ostrom, R. S., and Insel, P. A. (2004) The evolving role of lipid rafts and caveolae in G protein-coupled receptor signaling: implications for molecular pharmacology. *Br. J. Pharmacol.* **143,** 235–245
75. Patel, H. H., Murray, F., and Insel, P. A. (2008) G-protein-coupled receptor-signaling components in membrane raft and caveolae microdomains. *Handb. Exp. Pharmacol.* **186,** 167–184
76. Shenoy, S. K., and Lefkowitz, R. J. (2005) Receptor-specific ubiquitination of β-arrestin directs assembly and targeting of seven-transmembrane receptor signalosomes. *J. Biol. Chem.* **280,** 15315–15324
77. Tsvetanova, N. G., Irannejad, R., and von Zastrow, M. (2015) G protein-coupled receptor (GPCR) signaling via heterotrimeric G proteins from endosomes. *J. Biol. Chem.* **290,** 6689–6696
78. Fukuroda, T., Kobayashi, M., Ozaki, S., Yano, M., Miyauchi, T., Onizuka, M., Sugishita, Y., Goto, K., and Nishikibe, M. (1994) Endothelin receptor subtypes in human *versus* rabbit pulmonary arteries. *J. Appl. Physiol.* **76,** 1976–1982
79. Gangadharan, V., Nohe, A., Caplan, J., Czymmek, K., and Duncan, R. L. (2015) Caveolin-1 regulates P2X7 receptor signaling in osteoblasts. *Am. J. Physiol. Cell Physiol.* **308,** C41–C50
80. Choi, R. C., Chu, G. K., Siow, N. L., Yung, A. W., Yung, L. Y., Lee, P. S., Lo, C. C., Simon, J., Dong, T. T., Barnard, E. A., and Tsim, K. W. (2013) Activation of UTP-sensitive P2Y2 receptor induces the expression of cholinergic genes in cultured cortical neurons: a signaling cascade triggered by $Ca^{2+}$ mobilization and extracellular regulated kinase phosphorylation. *Mol. Pharmacol.* **84,** 50–61
81. Shenoy, S. K., and Lefkowitz, R. J. (2011) β-Arrestin-mediated receptor trafficking and signal transduction. *Trends Pharmacol. Sci.* **32,** 521–533
82. Premont, R. T., and Gainetdinov, R. R. (2007) Physiological roles of G protein–coupled receptor kinases and arrestins. *Annu. Rev. Physiol.* **69,** 511–534
83. Ebisuya, M., Kondoh, K., and Nishida, E. (2005) The duration, magnitude and compartmentalization of ERK MAP kinase activity: mechanisms for providing signaling specificity. *J. Cell Sci.* **118,** 2997–3002
84. Kubale, V., Abramović, Z., Pogacnik, A., Heding, A., Sentjurc, M., and Vrecl, M. (2007) Evidence for a role of caveolin-1 in neurokinin-1 receptor plasma-membrane localization, efficient signaling, and interaction with β-arrestin 2. *Cell Tissue Res.* **330,** 231–245
85. Sato, S., Fujita, N., and Tsuruo, T. (2000) Modulation of Akt kinase activity by binding to Hsp90. *Proc. Natl. Acad. Sci. U.S.A.* **97,** 10832–10837
86. Ivaska, J., Nissinen, L., Immonen, N., Eriksson, J. E., Kähäri, V. M., and Heino, J. (2002) Integrin α2β1 promotes activation of protein phosphatase 2A and dephosphorylation of Akt and glycogen synthase kinase 3β. *Mol. Cell. Biol.* **22,** 1352–1359
87. Xu, W., Yuan, X., Jung, Y. J., Yang, Y., Basso, A., Rosen, N., Chung, E. J., Trepel, J., and Neckers, L. (2003) The heat shock protein 90 inhibitor geldanamycin and the ErbB inhibitor ZD1839 promote rapid PP1 phosphatase-dependent inactivation of AKT in ErbB2 overexpressing breast cancer cells. *Cancer Res.* **63,** 7777–7784
88. McMahon, H. T., and Boucrot, E. (2011) Molecular mechanism and physiological functions of clathrin-mediated endocytosis. *Nat. Rev. Mol. Cell Biol.* **12,** 517–533
89. Camden, J. M., Schrader, A. M., Camden, R. E., González, F. A., Erb, L., Seye, C. I., and Weisman, G. A. (2005) P2Y2 nucleotide receptors enhance α-secretase-dependent amyloid precursor protein processing. *J. Biol. Chem.* **280,** 18696–18702
90. Weisman, G. A., Ajit, D., Garrad, R., Peterson, T. S., Woods, L. T., Thebeau, C., Camden, J. M., and Erb, L. (2012) Neuroprotective roles of the P2Y2 receptor. *Purinergic Signal.* **8,** 559–578
91. Weisman, G. A., Camden, J. M., Peterson, T. S., Ajit, D., Woods, L. T., and Erb, L. (2012) P2 receptors for extracellular nucleotides in the central nervous system: role of P2X7 and P2Y2 receptor interactions in neuroinflammation. *Mol. Neurobiol.* **46,** 96–113
92. Gentry, P. R., Sexton, P. M., and Christopoulos, A. (2015) Novel allosteric modulators of G protein-coupled receptors. *J. Biol. Chem.* **290,** 19478–19488
93. Dohlman, H. G. (2015) Thematic minireview series: new directions in G protein-coupled receptor pharmacology. *J. Biol. Chem.* **290,** 19469–19470

# Caveolin-1 Regulates the $P2Y_2$ Receptor Signaling in Human 1321N1 Astrocytoma Cells

Namyr A. Martinez, Alondra M. Ayala, Magdiel Martinez, Freddyson J. Martinez-Rivera, Jorge D. Miranda and Walter I. Silva

*J. Biol. Chem. 2016, 291:12208-12222.*
*doi: 10.1074/jbc.M116.730226 originally published online April 18, 2016*

---